

Description of Five New *Loma* (Microsporidia) Species in Pacific Fishes with Redesignation of the Type Species *Loma morhua* Morrison & Sprague, 1981, Based on Morphological and Molecular Species-Boundaries Tests

AMANDA M. V. BROWN,^a MICHAEL L. KENT^b and MARTIN L. ADAMSON^a

^aDepartment of Zoology, University of British Columbia, 6270 University Boulevard, Vancouver, British Columbia, Canada V6T 1Z4, and

^bDepartment of Microbiology, Oregon State University, 220 Nash Hall, Corvallis, Oregon 97331, USA

ABSTRACT. Five new species of *Loma* were described from five Pacific fishes using light-microscopic and ultrastructural features along with phylogenetic analysis of the gene sequences of ribosomal RNA (rRNA) and elongation factor 1-alpha. Morphological data revealed both qualitative and quantitative differences in developmental stages and timing, vesicles, xenoma features, and spore sizes with statistical support that differentiated *Loma pacificodae* n. sp. in Pacific cod, *Loma wallae* n. sp. in walleye pollock, *Loma kenti* n. sp. in Pacific tomcod, *Loma lingcodae* n. sp. in lingcod, and *Loma richardi* n. sp. in sablefish from each other and other species in the genus. Phylogenetic analyses combined with monophyly tests supported species designations, but with low resolution in two cases perhaps due to rRNA paralogs or recent speciation. *Loma branchialis* in haddock was shown to be separate from *Loma morhua* in Atlantic cod, thereby making *L. morhua*, and not *L. branchialis*, the type species. A species from brook trout was shown to be a separate species from *Loma salmonae*, not a variant strain selected in the laboratory. By comparison with gadid host phylogeny, these *Loma* species appear to have coevolved with their hosts, first colonizing the Pacific basin about 12 million years ago.

Key Words. *Anoplopoma fimbria*, EF1-alpha, *Gadus macrocephalus*, *Gadus morhua*, *Loma branchialis*, monophyly test, *Ophiodon elongatus*, phylogeny, rDNA, xenoma.

LOMA Morrison & Sprague, 1981 species, like other microsporidia, are tiny, single-celled, intracellular parasites that undergo a number of vegetative divisions in contact with their host's cell cytoplasm or in sacs created by the parasite or host, eventually forming infective spores (for review see Cali and Takvorian 1999). They are typically recognized by the formation of spore-filled, cyst-like nodules consisting of highly modified host-parasite complexes called "xenomas" in the gills or other vascularized tissues. Xenomas and spores may occlude blood vessels, causing severe inflammatory response or death (Becker and Speare 2007; Hauck 1984; Kent and Speare 2005; Lovy, Wright, and Speare 2007; Speare, Brackett, and Ferguson 1989). Some species cause serious losses to wild and cultured fisheries, for example *Loma salmonae* (Putz, Hoffman & Dunbar, 1965) Morrison & Sprague, 1981 in salmon and trout *Oncorhynchus* spp., *Loma branchialis* (Nemeczek, 1911) Morrison & Sprague, 1981 in Atlantic cod *Gadus morhua* L., and *Loma camerounensis* Fomena, Coste & Bouix, 1992 in tilapia *Oreochromis niloticus* (L.) (Fomena et al. 1992; Kent et al. 1989; Khan 2009; Shaw and Kent 1999). Five undescribed *Loma*-like infections were reported in British Columbia, Canada (Kent et al. 1998) infecting Pacific cod *Gadus macrocephalus* Tilesius, 1810, walleye pollock *Theragra chalcogramma* (Pallas, 1814) Lucas, 1899, Pacific tomcod *Microgadus proximus* (Girard, 1854) Gill, 1865, lingcod *Ophiodon elongatus* Girard, 1854, and sablefish *Anoplopoma fimbria* (Pallas, 1814) Ayres, 1859, four of these being commercially important.

Typically, *Loma* species are described based on host species, spore size, xenoma size and features, timing and formation of the parasitophorous vacuole (PV), and form and abundance of episporontal inclusions (Lom 2002; Lom and Pekkarinen 1999). Historically, spores were a key diagnostic feature, but today they are usually considered inadequate based on significant statistical overlap among species (Azevedo and Matos 2002; Bekhti and Bouix 1985; Kabata 1959; Morrison and Sprague 1981a; Shaw et al. 1997). Furthermore, other morphological features often overlap between species-pairs that have been shown by transmission studies to be non-infective to reciprocal hosts, and therefore,

almost certainly genetically isolated species (Lom 2002; Shaw and Kent 1999; Shaw et al. 1997, 2000c). Thus, the present study attempted to better characterize features traditionally used but often inadequately examined in *Loma* species, including merogonial and sporogonial stages, developmental divisions, the material in the xenoma cytoplasm that contributes to the sac around the parasite, and episporontal inclusions. Morphological and genetic features were used to describe five new *Loma* species, *Loma pacificodae* n. sp., *Loma wallae* n. sp., *Loma kenti* n. sp., *Loma lingcodae* n. sp., and *Loma richardi* n. sp. and to help clarify appropriate designation of type species by distinguishing *L. branchialis* from *Loma morhua* Morrison & Sprague, 1981. Comparative pathology, prevalence, ultrastructural, and developmental features, and their biological implications were also described. For molecular comparison, two independent genetic loci were chosen because of their potential sequence variation and comparability with published studies: ribosomal RNA (rRNA) and partial elongation factor 1-alpha (EF-1 α) genes (Kamaishi et al. 1996; Vossbrinck and Debrunner-Vossbrinck 2005).

MATERIALS AND METHODS

Specimen collection. New *Loma* species from Pacific fishes were collected by trawling off the coast of Vancouver Island, British Columbia, Canada from Juan de Fuca Strait (48.15°N, 124.00°W), to the region off Barkley Sound (48.50°N, 125.20°W), and up to Queen Charlotte Sound (51.20°N, 129.00°W). This provided a geographic range for comparisons among these species in sympatry, each of which, if valid, would be expected to possess characters with a statistically separate mean with agreement across the sampled geographic isolates (Templeton 1994; Wheeler and Meier 2000). *Loma salmonae* were collected from various species of Pacific salmon and rainbow trout (*Oncorhynchus* spp.) captured by hook and line, seine, or trawling from bays, rivers, and coastal regions in British Columbia, or were donated from farms and hatcheries in British Columbia, Idaho, California, and Chile. Other *L. salmonae* specimens were obtained from laboratory-reared salmon at the Pacific Biological Station, Nanaimo, Canada (as described in Shaw, Kent, and Adamson 2000a). *Loma embiotociae* Shaw, Kent, Docker, Brown, Devlin & Adamson, 1997 from shiner perch *Cymatogaster aggregata* Gibbons, 1854 were collected from various locations in British Columbia. *Loma morhua* and

Corresponding Author: A. Brown, Department of Zoology, University of British Columbia, 6270 University Boulevard, Vancouver, British Columbia, Canada V6T 1Z4—Telephone number: +778 865 8858; FAX number: +604 822 2416; email: abrown@zoology.ubc.ca

Table 1. Primers used to amplify and sequence partial rDNA and elongation factor 1-alpha (*EF-1 α*), listed 5'-3'.

Primer	Sequence	Position	Source
rDNA forward			
M5P	CAC CAG GTT GAT TCT GCC	-18 to 0	Docker et al. (1997b) ^a
Seq1f	CGT TGT AGT TCT AGC AGT	701–718	From M. F. Docker
L7f	ATT AGT GAG ACC TCR GCC	983–1,000	Docker et al. (1997a)
580f	GAT AYA AGT CGT AAC AAG	1,299–1,316	This study
L1	CTG GAT CAG ACC GAT TTA TAT	1,339–1,359	Docker et al. (1997a)
rDNA reverse			
SeqR	AAC AGG GAC KYA TTC ATC	1,198–1,215	This study
1492r	GGT TAC CTT GTT ACG ACT T	1,304–1,450	Baker et al. (1995)
L3R	CGA CTC CTG CAC ATT TCG	1,590–1,610	This study
L2	ATG ACA TCT CAC ATA ATT GTG	1,590–1,610	Docker et al. (1997a)
580r	GGT CCG TGT TTC AAG ACG G	1,830–1,848	Vossbrinck et al. (1987)
<i>EF-1α</i> forward			
EFZ	TTG CTT CAT TGG NCA CGT MGA	32–52	This study
EFE	AGA AAG AGG TAG WGG TWC	143–160	This study
EFV	GTA CAT ATC GTG GTA TTA C	198–217	This study
<i>EF-1α</i> reverse			
EFD	TGC ACC TGT ACT ACY CTN CCN GT	806–828	This study
EFW	AAG TCA CAT TTT CAC CTT T	1,203–1,221	This study
EGF	AGT TTC CAT KAC RAC TTG	1,241–1,259	This study

Reference sequences: rDNA *Loma salmonae* reference sequence; *EF-1 α* *Glugea plecoglossi* (GenBank D84253).

^aDocker et al. (1997b) called this 18eMIC.

L. branchialis were collected from heads of Atlantic cod and haddock, respectively, from a market in Halifax, Nova Scotia, Canada. These fish were caught aboard commercial vessels in the area approaching Halifax harbour. Other specimens of *L. morhua* from Atlantic cod collected near St. John's, Newfoundland, Canada were provided by D. Barker (Marine Institute, Memorial University). Gills from a *Loma*-like infection (hereafter referred to as *Loma* sp. BRO) in laboratory-reared brook trout *Salvelinus fontinalis* (Mitchill, 1814) Jordan & Crossman, 1878 from the Atlantic Veterinary College, Prince Edward Island, Canada were provided by J. G. Sánchez-Martínez (Atlantic Veterinary College, Prince Edward Island, Canada). Gills from an undescribed *Loma* species from Australian surf bream, *Acanthopagrus australis* (Günther, 1859) in Queensland, Australia were provided by R. Adlard (hereafter referred to as *Loma* sp. AUS).

Tissues were examined in wet mounts as soon as possible postmortem for the presence of xenomas (100–400X magnification). Where possible, positive infections were examined at higher magnification for the presence of spores. Fresh, sterile blades and forceps thoroughly washed, soaked in 10% bleach solution, and flame-sterilized between specimens were used to prevent cross-contamination. For a small number of specimens single xenomas were isolated by excision using fresh, sterile blades and then examined under a cover slip at 400X magnification to

confirm the absence of other xenomas in adjacent tissue.

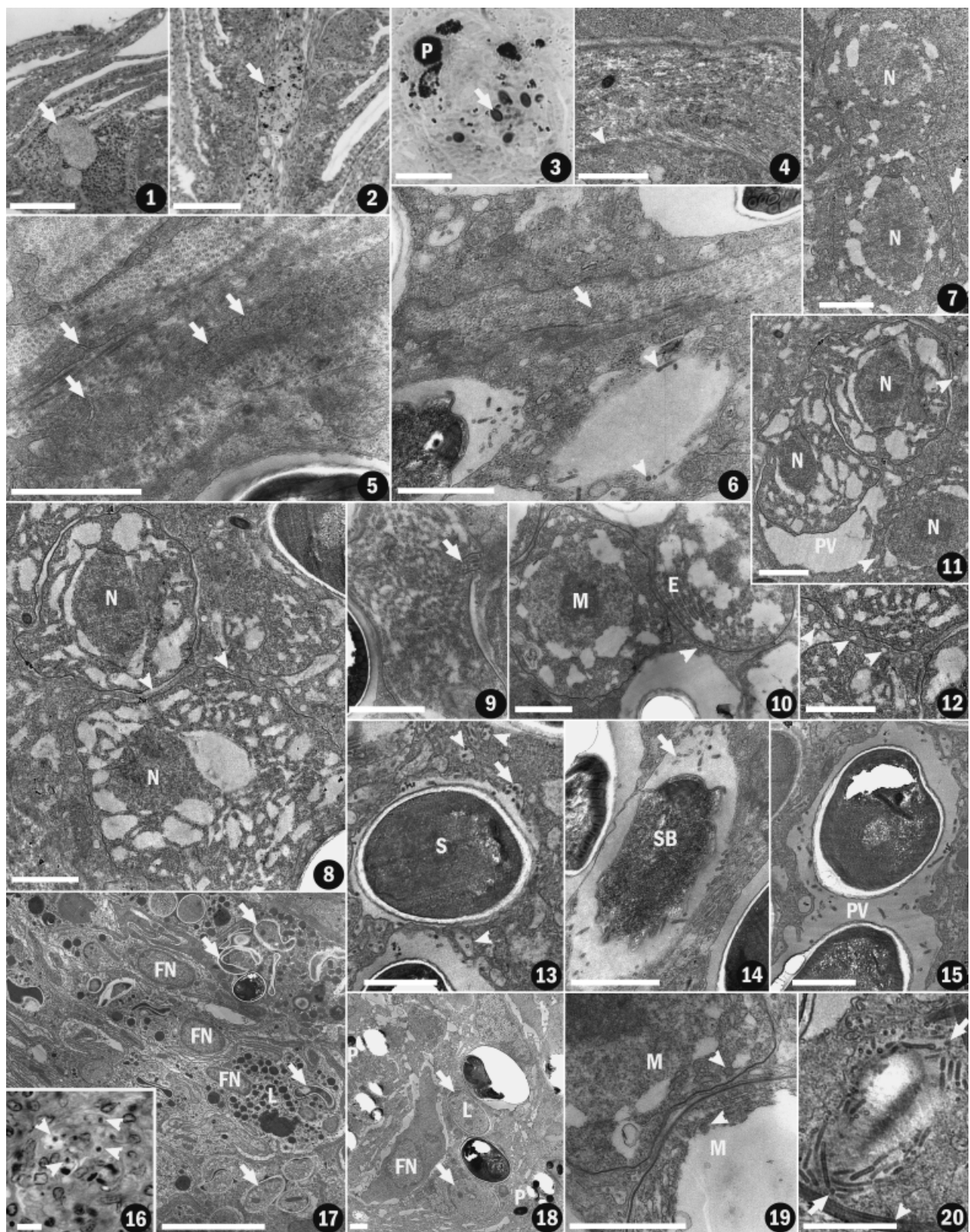
Tissue fixation and preparation. Tissues for DNA analysis were fixed in 95% ethanol or sometimes homogenized from fresh or frozen tissue and run through Percoll (Sigma, Ronkonkoma, NY) gradients to purify spores. Tissues for histological examination were fixed in Davidson's solution then embedded in paraffin, sectioned, and stained with haematoxylin and eosin. Tissue for transmission electron microscopy was fixed in 4% (v/v) glutaraldehyde for 12–24 h, soaked in either Millonig's solution or Sörensen's solution (0.1 M, pH 6.8) for 24 h, post-fixed in 1% (w/v) osmium tetroxide for 1 h, then embedded in standard Spurr's resin. Ultrathin sections were lifted onto copper grids and stained with 2% (w/v) aqueous uranyl acetate followed by standard Reynold's lead citrate.

Prevalence and intensity measurement. Gills were examined for xenomas at low power and then at highest power (1,000X) to confirm infections. About 6–8 cm of gill tissue from a single gill arch were examined from each fish. Prevalence (i.e. percent of hosts having xenomas in the gills) was determined by light microscopy from both wet mounts and histological sections. Intensity of infection was determined by counting the number of well-oriented gill filaments and the number of xenomas on those filaments, giving a value of number of xenomas per gill filament (xpf) (see Speare, Arsenault, and Buote 1998).

Fig. 1–20. Light (1–3, 16) and transmission electron micrographs (4–15, 17–20) of *Loma pacificodae* n. sp. from Pacific cod *Gadus macrocephalus*. **1, 2.** Xenomas (arrows) of two types: round xenomas at base of secondary lamella of gill, and oblong xenoma in central venous sinus of gill. **3.** Spores (arrow) in gonads with dark pigment granules (P) of melanomacrophage. **4, 5.** Xenoma wall showing granular material interspersed with collagenous fibres over a smooth plasmalemma (arrowhead) or interdigitated plasmalemma (arrows). **6.** Collagen intrusion (arrow) into middle of xenoma with tubules (arrowheads) visible in parasitophorous vacuoles. **7, 8.** Meronts: merogonal plasmodium undergoing binary fission within host rough endoplasmic reticulum (RER) (arrow) and highly vacuolated meronts or merogonal plasmodia with early parasitophorous vacuole formation (arrowheads). N, nuclei. **9.** Oblong, thick-walled, sporogonal plasmodium with a tubule-filled invagination (arrow). **10.** Early meront (M) within host RER and later smooth-walled stage accumulating tubule-filled vesicles (arrowhead) at surface and containing developing stacked ER cisternae (E). **11, 12.** Parasitophorous vacuole (PV) formation around highly vacuolated meronts or merogonal plasmodia with thickened surface coats (N, nuclei) showing small light, empty vesicles (arrowheads) gathered around meront surfaces. **13, 14.** Tubule-filled vesicles (arrowheads) and tubules (arrows) in PV space of early spore (S) and sporoblast (SB). **15, 16, 17, 18.** Host response showing granulomas with spores engulfed by host phagocytes (arrowheads), spores being engulfed and digested (arrows) nearby fibroblast nuclei (FN) and lysosomes (L), and pigment granules (P) in the ovaries. **19.** Detail of merogonal stages (M) showing double membrane-bound vesicles (arrowheads) with slightly dark contents, about 75–90 nm. **20.** Graze-cut of PV space showing tubules oriented about the longitudinal poles (arrowheads). Scale bars: 100 μ m (1–2) and 10 μ m (3, 16–17) and 1 μ m (4–15, 18–20).

Morphological measurements and statistical analysis. Xenomas were measured from histological and resin-embedded sections by light microscopy (400 and 1,000X) using a calibrated ocular micrometre. Xenomas not packed with spores and without

sharp walls were not counted. Xenomas were also not counted if they appeared to be in “graze cut” (i.e. a cut through just an edge) as recognized by the lack of sharpness of the wall or an unusually thick wall and the absence of a host-nucleus.



Spores were measured from histological and resin-embedded sections and ethanol-fixed material in wet mount by photographing under light microscopy (1,000X). Photographic negatives were scanned at 2,000 dpi, opened in Adobe Photoshop 6.0, enlarged, and measured with a ruler on screen. Scale bars were calculated for original photographs using a calibrated ocular micrometre with estimated accuracy of $\pm 0.05 \mu\text{m}$ and these were used to calculate sizes of spores using the screen enlargement factor. Spore shrinkage due to fixation was estimated for each species by calculating the spore size ratio from each pair of fixation methods (e.g. mean fresh spore size divided by mean resin-embedded spore size). Shrinkages of length and width were calculated separately. The resulting shrinkage factors were used to convert spore sizes from fixed material into estimated fresh spore sizes where fresh spore sizes were unavailable.

Other ultrastructural features were measured after being photographed on a Zeiss 10C Transmission Electron Microscope (Oberkochen, Germany). Negatives were scanned at 1,200 dpi and opened in Adobe Photoshop 6.0. Features were enlarged for measurement and structures were measured on screen. Scale bars were calculated for original photographs using magnification factors calculated for the electron microscope and these were used to calculate sizes of structures using the screen enlargement factor. Developmental stages were recognized and defined as in previous studies (Lom and Nilsen 2003; Lom and Pekkarinen 1999). Round structures, such as vesicles, meronts, and spores that appeared to be in graze cuts were not counted. Spores were easily recognized as middle longitudinal axis cuts by internal features, such as complete rows of round polar filaments. Vesicles were considered to be associated with a given cell (i.e. destined to contribute material to the parasite cell surface), if found within a space delimited by a line drawn halfway between the surface of the cell and adjacent cells.

Statistical support for morphological differences was assessed by either parametric (ANOVA and Tukey's test or two-sample *t*-test and *F*-tests) or non-parametric methods (Kruskal–Wallis and Nemenyi tests or *F*-test and Mann–Whitney *U*-test using the normal approximation where necessary) following evaluation for normal fit using the Shapiro–Wilk normality test followed by Holm–Bonferroni correction in PAST version 2.01 (Hammer, Harper, and Ryan 2001).

DNA isolation. Up to 60 mg of ethanol-fixed tissue was soaked for 15 min in lysis buffer (10 mM Tris, 1 mM EDTA, 10 mM NaCl, 1% [w/v] SDS) to remove excess ethanol. Purified spore concentrates required bead beating (Docker et al. 1997a). Tissue or spores were then digested in 5–10X volume lysis buffer with 0.5 mg/ml proteinase K (Sigma) for 4–6 h at 37 °C in a rotating incubator. DNA was extracted once with phenol, twice with phenol:chloroform:isoamyl alcohol (25:24:1), once with chloroform, then precipitated in cold 95% ethanol, washed twice with 70% ethanol, and vacuum dried. The pellet was resuspended in 40 µl distilled water and stored for use at –20 °C.

Polymerase chain reaction (PCR) and DNA sequencing. Genomic DNA was amplified in 25-µl reactions using 0.3–0.8 µg genomic DNA, standard PCR buffer (Boehringer Mannheim, Mannheim, Germany), 2.5 mM MgCl₂, and 0.2 mM, dNTP, 15 pmol of each primer, and 1–3 U of Taq DNA polymerase (Boehringer Mannheim). Reactions were run in a Perkin Elmer Cetus DNA Thermal Cycler 480 (Perkin-Elmer Corporation, Norwalk, CT) with conditions: 1 min 95 °C, 35 cycles of 95 °C 50 s, 54 °C 30 s (or as low as 50 °C for difficult amplifications), 72 °C 90 s, 5 min 72 °C. Primers (Table 1) were created based on conserved regions from microsporidian sequences from GenBank. Polymerase chain reaction products were run in 1.5% agarose Tris-borate-EDTA or Tris-acetate-EDTA gels to visualize products. The desired product was gel-excised, freeze-thaw extracted

or β-agarase digested to remove agarose and then sequenced directly or after cloning.

Products for cloning were isolated in 0.8% agarose and cleaned for ligation using Ultraclean15 MOBIO DNA Purification Kit (BIO/CAN Scientific Inc., Mississauga, ON) and ligated and cloned using the TOPO TA Cloning PCR Version 2.1 (Invitrogen Corp., Carlsbad, CA), and screened in 10-µl PCR reactions using Taq DNA Polymerase (Invitrogen Corp.) with standard reagents and screening primers M13-20 and M13 Rev (conditions: 94 °C for 2 min, 34 cycles of 92 °C for 45 s, 55 °C for 45 s 72 °C for 1 min 30 s, followed by 72 °C for 5 min). Positive clones from master plates were grown in 3 ml of standard lysogeny broth culture with 50 mM ampicillin by shaking at 220 rpm at 37 °C overnight then isolated using the Rapid Plasmid Miniprep System (Gibco BRL, Gaithersburg, MD) following directions of the manufacturer.

Sequencing was performed on an ABI PRISM 377 DNA automated sequencer using BigDye Terminator Version 3.1 fluorescent dye-labelled terminators with forward and reverse primers and PCR conditions as recommended for the Taq terminators. Polymerase chain reaction products were sequenced in both directions and wherever possible, multiple PCR products and multiple clones were sequenced to check for Taq or sequencer errors.

Phylogenetic analysis. *Loma* sequences were easily aligned by eye using ESEE 3.2s (Eyeball SEquence Editor, Eric Cabot 1998), except for parts of the ITS ribosomal DNA (rDNA), which were aligned with the help of CLUSTAL W (version 1.74, Thompson, Higgins, and Gibson 1994) allowing for frequent transitions between closely related taxa. Sequencing directly from PCR products sometimes produced sequences having two different nucleotide signals at almost every site after a stretch of normal single nucleotide signals. In such cases, Flip Analyzer in REALEM Version 1.01 (Brown 2005; Brown and Adamson 2006) was used to extract single sequences. Sequencing directly from PCR products also sometimes produced polymorphic sites. Where valid polymorphisms could not be distinguished from sequencing artefacts (i.e. background contamination or sequencer software error), sequencing was repeated.

Phylogenetic analysis was performed in PAUP* Version 4.0b10 (Phylogenetic Analysis Using Parsimony; Swofford 2001) using maximum parsimony (MP), minimum evolution (ME) using the distance logDet/paralink model and maximum likelihood (ML) with heuristic search, random stepwise sequence addition, and TBR branch swapping with 10 repetitions. Maximum likelihood analysis was performed by first estimating the best-fit model of evolution for each data set using the Akaike Information Criterion method (Akaike 1974) in Modeltest Version 3.06 (Posada and Crandall 1998). Maximum likelihood heuristic searches were run using the best-fit model and parameters estimated from the data to generate a starting neighbour-joining tree under ML and parameters were re-estimated before heuristic ML searches. Bootstrap resampling was done with 1,000 replicates reported on 50% majority rule trees for MP, ME, and ML or for ML with larger data sets, 100 replicates using faststep searches. Analyses were performed to analyse the effects of removing gaps, removing ambiguous characters, adding indel information using Gap Matrix in REALEM, or including polymorphic characters by encoding polymorphic data using the “AND” rather than “OR” definition of multistate characters in MP analyses. Recombination tests were performed using Splits-Tree (Huson 1998) and LARD Version 2.2 (Holmes, Worobey, and Rambaut 1999).

Additional analyses were performed with other sequences from GenBank chosen based on BLAST (NCBI) similarity to *Loma* species and on relative completeness of rDNA sequence. For these analyses, a single *Loma* sequence from each species from the

Table 2. Comparison of morphological features among *Loma* species from this study.

	Mean	Range	SD	n	Significant differences
Xenoma size (μm)					Zcrit _{0.05,∞} 1.645, Ucrit _{0.05,1,n1n2} 2.47
<i>L. pacificodae</i> n. sp. cvS	120.1	47.0–226.2	50.3	43	W (Z = 2.919) W (U = 286)
<i>L. pacificodae</i> n. sp. 2nd	47.3	29.0–87.0	20.5	15	
<i>L. wallae</i> n. sp.	82.9	27.8–168.8	43.0	25	
<i>L. kentii</i> n. sp.	142.3	104.4–211.7	34.6	8	
<i>L. lingcodae</i> n. sp.	37.4	18.0–81.8	14.9	56	
<i>L. richardi</i> n. sp.	33.1	31.3–35.4	1.6	5	qcrit _{0.05,6,5} 3.977/Qcrit _{0.05,4} 2.639 R (q = 7.929)/L (Q = 4.263), R (Q = 6.884)
Vesicle size (μm)/tubules per vesicle					
<i>L. pacificodae</i> n. sp.	0.203/3.0	0.106–0.354/1–8	0.067/1.8	16/33	
<i>L. wallae</i> n. sp.	0.26/4.0	0.178–0.431/1–10	0.075/2.4	10/23	R (q = 6.083)/R (Q = 5.225)
<i>L. kentii</i> n. sp.	0.715/0	0.321–1.733/—	0.418/—	15/16	L (q = 7.798) R (q = 6.921)/R (Q = 2.922)
<i>L. lingcodae</i> n. sp.	0.277/16.1	0.176–0.441/3–11	0.061/2.1	19/28	
<i>L. richardi</i> n. sp.	0.658/15.6	0.324–1.250/2–50	0.272/10.7	16/20	
Vesicles per sporoblast/vesicles per sporoblast					qcrit _{0.05,30,5} 4.102/Qcrit _{0.05,5} 2.807
<i>L. pacificodae</i> n. sp.	8.0/3.8	3–11/2–7	2.6/1.8	7/10	W (q = 9.427), R (q = 5.582)
<i>L. wallae</i> n. sp.	1.9/3.6	0–4/1–13	1.3/3.2	9/14	L (q = 8.429)
<i>L. kentii</i> n. sp.	3.5/2.2	2–6/0–5	1.3/1.5	8/12	L (q = 5.6)/L (Q = 3.129)
<i>L. lingcodae</i> n. sp.	7.0/4.8	4–11/2–7	2.1/1.7	9/10	R (q = 4.528)
<i>L. richardi</i> n. sp.	3.5/2.5	2–5/1–5	1.3/1.4	4/8	
Tubules per sporoblast/tubules per sporoblast					qcrit _{0.05,18,4} 3.997/Qcrit _{0.05,5} 2.807
<i>L. pacificodae</i> n. sp.	19.3/9.0	1–36/2–22	14.3/5.5	4/12	R (q = 7.544)/R (Q = 4.627)
<i>L. wallae</i> n. sp.	8.0/5.9	2–17/2–13	5.1/4.0	7/10	R (q = 9.859)/R (Q = 5.4)
<i>L. kentii</i> n. sp.	0/0	—	—	8/10	
<i>L. lingcodae</i> n. sp.	17.0/11.8	6–34/1–27	8.6/7.1	7/23	R (Q = 4.462)
<i>L. richardi</i> n. sp.	90.3/52.0	63–152/30–78	41.5/15.1	4/16	
Polar filament turns					qcrit _{0.05,30,5} 4.102
<i>L. pacificodae</i> n. sp.	17.9	16–22	1.8	14	K (q = 4.575), L (q = 5.704), R (q = 8.699)
<i>L. wallae</i> n. sp.	18.6	16–21	2.1	5	K (q = 6.893), L (q = 5.792), R (q = 8.205)
<i>L. kentii</i> n. sp.	14.8	14–16	0.7	12	
<i>L. lingcodae</i> n. sp.	15.0	14–16	0.9	6	
<i>L. richardi</i> n. sp.	13.5	11–15	1.5	6	
Spore size (μm) in Spur's resin					P-value at 0.05
<i>L. pacificodae</i> n. sp.	3.48 × 1.95	2.84–3.95 × 1.68–2.34	0.41 × 0.21	12	/W (p = 0.0283)
<i>L. wallae</i> n. sp.	3.37 × 1.81	2.85–3.64 × 1.68–1.96	0.24 × 0.08	11	
<i>L. kentii</i> n. sp.	2.94 × 1.52	2.63–3.22 × 1.39–1.75	0.20 × 0.10	12	
<i>L. lingcodae</i> n. sp.	3.00 × 1.65	2.78–3.33 × 1.39–1.87	0.20 × 0.14	10	R (p = 1.05 × 10 ⁻⁷)/R (p = 0.00302)
<i>L. richardi</i> n. sp.	3.81 × 1.93	3.38–4.12 × 1.67–2.49	0.24 × 0.25	10	
Spore size (μm) converted to fresh size equivalents					qcrit _{0.05,7} 3.038/Qcrit _{0.05,7} 3.038
<i>L. pacificodae</i> n. sp.	5.28 × 2.63	4.35–5.94 × 2.08–3.18	0.51 × 0.29	22	K (Q = 4.043), L (Q = 5.363), A (Q = 3.409)/K (Q = 3.563), L (Q = 3.852)
<i>L. wallae</i> n. sp.	5.12 × 2.53	4.29–5.71 × 2.26–2.96	0.34 × 0.17	21	K (Q = 3.118), L (Q = 4.394), A (Q = 4.244), H (Q = 3.169)/A (Q = 3.409), H (Q = 4.049), L (Q = 3.176)
<i>L. kentii</i> n. sp.	4.42 × 2.21	3.95–5.01 × 1.87–4.37	0.31 × 0.48	24	R (Q = 4.943), A (Q = 7.620), H (Q = 6.816)/A (Q = 6.541), H (Q = 7.498)
<i>L. lingcodae</i> n. sp.	4.41 × 2.15	3.92–5.01 × 1.78–2.54	0.27 × 0.19	27	R (Q = 5.963), A (Q = 9.077), H (Q = 8.406)/A (Q = 6.925), H (Q = 7.971)
<i>L. richardi</i> n. sp.	5.73 × 2.62	5.01–6.20 × 2.27–3.38	0.37 × 0.34	10	
<i>L. morhua</i>	5.98 × 3.24	5.29–6.49 × 2.63–3.68	0.37 × 0.27	24	
<i>L. branchialis</i>	5.70 × 3.14	3.89–6.38 × 2.70–3.68	0.48 × 0.25	35	

cvS, *Loma pacificodae* n. sp. in the central venous sinus; 2nd, *L. pacificodae* n. sp. in the secondary lamellae; SD, standard deviation; n, number measured.

Significant differences: Letter symbols indicate a species whose feature is statistically significantly different (W, *Loma wallae* n. sp.; K, *Loma kentii* n. sp.; L, *Loma richardi* n. sp.; A, *Loma morhua* n. sp. from Atlantic cod; H, *Loma branchialis* from haddock) and value in parentheses following letter symbol indicates significance test result for critical values lower than probability 0.05 from multivariate analysis (following Tukey's test, indicated by Q) or non-parametric (Kruskal–Wallis and F-test followed by Nemenyi test, indicated by Q methods, or for xenoma size and resin-embedded spore sizes, Mann–Whitney U-tests or two-sample t-test, indicated by Z or U, or p, respectively).

Table 3. Prevalence of *Loma* species showing difference between estimates from histological sections and wet mounts (parentheses = number examined).

Species	Prevalence (%)		
	Histology	Wet mount	Combined
<i>L. pacificodae</i> n. sp.	41.3 (121)	26.0 (154)	32.6 (227)
<i>L. wallae</i> n. sp.	35.6 (45)	24.4 (131)	28.3 (145)
<i>L. kenti</i> n. sp.	5.3 (57)	14.4 (409)	14.4 (419)
<i>L. morhua</i>	—	4.4 (427)	4.4 (427)
<i>L. branchialis</i>	—	6.5 (232)	6.5 (232)
<i>L. lingcodae</i> n. sp.	16.7 (156)	21.1 (199)	21.4 (210)
<i>L. richardi</i> n. sp.	3.9 (128)	13.2 (197)	13.2 (197)
<i>L. embiotociae</i>	—	8.5 (94)	8.5 (94)
<i>L. salmonae</i>	—	12.5 (8)	12.5 (8)

present study was produced by determining the most common nucleotide at each position. Sequences were aligned by eye and with the help of CLUSTAL W, and areas of ambiguous alignment removed. To speed ML analyses, outgroup taxa with very high similarity were removed. Maximum parsimony, ME and ML analyses were performed as described above.

Monophyly constraints and approximately unbiased (AU) tests. Statistical tree-comparison hypothesis testing (Shimodaira and Hasegawa 2001) was used because although all members of a species would be expected to form a monophyletic clade (Mallet 1995; Sites and Crandall 1997), some sequences may fall outside the clade by chance alone. Hypothetical trees were created to constrain sequences into various monophyletic groups using TreeView Version 1.6.6 (Page 1996) by varying the position of parentheses on tree files. Constrained trees were added to the commands in PAUP* before heuristic distance searches. Constrained trees were inspected to ensure equal numbers of nodes and topological identity to that of unconstrained trees outside the modified clades to obey the assumptions of the statistical tests. Log likelihood values (lscores) were calculated for the set of shortest trees using the best-fit substitution model and parameters estimated for the data using Modeltest. Lscores and overall tree likelihoods from unconstrained and constrained trees were then analysed using CONSEL version 0.1f (Shimodaira and Hasegawa 2001), which compares trees using the AU test and other similar tests (see Goldman, Anderson, and Rodrigo 2000; Shimodaira 2002; Shimodaira and Hasegawa 2001).

RESULTS

Loma pacificodae n. sp. (Fig. 1–20)

Morphology of *Loma pacificodae* n. sp. Infections were characterized by xenomas of the cell hypertrophy type with enlarged, branched, but not divided host nuclei found primarily in the gills, of two types, differing in shape and tissue origin: one elongate and located in the central venous sinus behind the efferent blood vessel arising from fibroblast connective tissue or lymph vessels, and the other round or septate and located at the base of the secondary lamellae arising from pillar cells (Fig. 1, 2), and differing in size (Table 2). Xenomas were also found in the gonads in more than half of infected hosts (Fig. 3), and in the spleen and heart in about half of the cases, sometimes in the gallbladder, and rarely in the liver and kidney. The xenoma wall consisted of a smooth or interdigitated plasmalemma covered by thick lucent, granular, amorphous material in one layer mixed with collagen fibres and fibroblast inclusions 1.5–2.0 µm thick (Fig. 4, 5). Collagenous material occurred in the middle of xenomas (Fig. 6). Developmental stages and spores were intermixed and nuclei were always unpaired. Uninucleate meronts had a thin surface glycocalyx coat

in direct contact with the xenoma cytoplasm undergoing binary fission within a host rough endoplasmic reticulum (RER) covering (Fig. 7). Merogonial plasmodia were highly vacuolated (Fig. 8). Sporogonial plasmodia were oblong and rounded with a smooth, thick glycocalyx coat enclosed within a PV of host origin (Fig. 9). Parasitophorous vacuole formation occurred before sporogony (Fig. 10, 11), apparently by coalescence of small, 60–200 nm membrane-bound vesicles (Fig. 12) and by coalescence of tubule-filled vesicles assembled around later stages (Fig. 13). Tubules were present in PV spaces before sporogony. Tubule-filled vesicles were small with few tubules per vesicle (Table 2) and numerous tubule-filled vesicles were associated with sporoblasts and spores (Table 2). Numerous tubules occurred in PV spaces of the sporoblast and spore (Table 2).

Spores were ovoid and slightly narrower at the anterior end with sub-apically situated anchoring disc with typical lamellar and vesicular polaroplasts, a singly coiled polar filament with 17.9 ± 0.9 turns (Table 2), and an exospore with fine ridges on the outer surface. Spores measured: fresh 5.5 (4.8–6.0) µm long \times 3.0 (2.7–3.2) µm wide ($n = 10$), frozen 4.6 (4.0–5.5) µm long \times 2.5 (2.0–3.0) µm wide ($n = 30$), formalin-fixed paraffin-embedded 3.58 ± 0.15 µm long \times 1.94 ± 0.15 µm wide ($n = 10$), and Spurr's resin-embedded 3.48 ± 0.23 µm long \times 1.95 ± 0.12 µm wide ($n = 12$). The posterior vacuoles were one-fourth of the spore volume. There were two spores per PV.

Ecology and pathology of *Loma pacificodae* n. sp. “Mean” prevalence was 32.6% ($n = 227$) (Table 3), and was lower north of $49^{\circ}7'N$ lat. Infections occurred in male and female hosts ranging in size from 34 to 61 cm with middle-sized to larger fish more often and most heavily infected. Intensity of infection ranged from one to four xenomas per gill arch to 59 xenomas in 30 primary lamellae = 2.0 xpf. Fish with heavy infections exhibited macroscopic changes: gills appeared pale and other organs (e.g. liver, spleen, or gonads) were occasionally discoloured and mottled in appearance. In one case the *Loma*-infected egg-filled ovaries were almost completely black, presumably from melanization, while other tissues were speckled with black spots. In histological sections, heavily infected organs showed signs of host defence: granuloma formation and subsequent changes in tissue structure (e.g. secondary lamellar fusion) once a xenoma was cleared. In severe cases about a third of secondary lamellae were fused, and in active infections granulomas were as common as intact xenomas. Typical granulomas had recognizable xenoma walls but few remaining recognizable spores (Fig. 16–18). Xenomas in the central venous sinus of primary lamellae showed signs of host response (i.e. sparsely distributed spores, phagocytes engulfing spores, and wall less defined or intact), whereas xenomas in the bases of secondary lamellae showed no or few signs of host response (i.e. wall sharp and intact, spores densely packed, and no signs of host cells in xenoma). Fibroblasts were seen infiltrating xenomas and spores were in various stages of being engulfed and digested (Fig. 17).

Loma wallae n. sp. (Fig. 21–29)

Morphology of *Loma wallae* n. sp. Xenomas were found primarily in the central venous sinus of gills in fibroblast connective tissue and were rounded oval in shape (Fig. 21), often septate or divided (Fig. 22), and medium-sized (Table 2). Xenomas or spores were found in ~80% of cases in the gallbladder, in more than half of cases in the gonads, in about half of cases in the spleen and heart, and rarely in liver and kidney. The xenoma wall consisted of a smooth plasmalemma covered by thick, lucent, granular, amorphous material in three layers with collagenous fibres and fibroblast inclusions, 2.5 µm thick (Fig. 23). Developmental stages and spores were intermixed and nuclei were always unpaired. Uninucleate meronts had a thin glycocalyx coat without

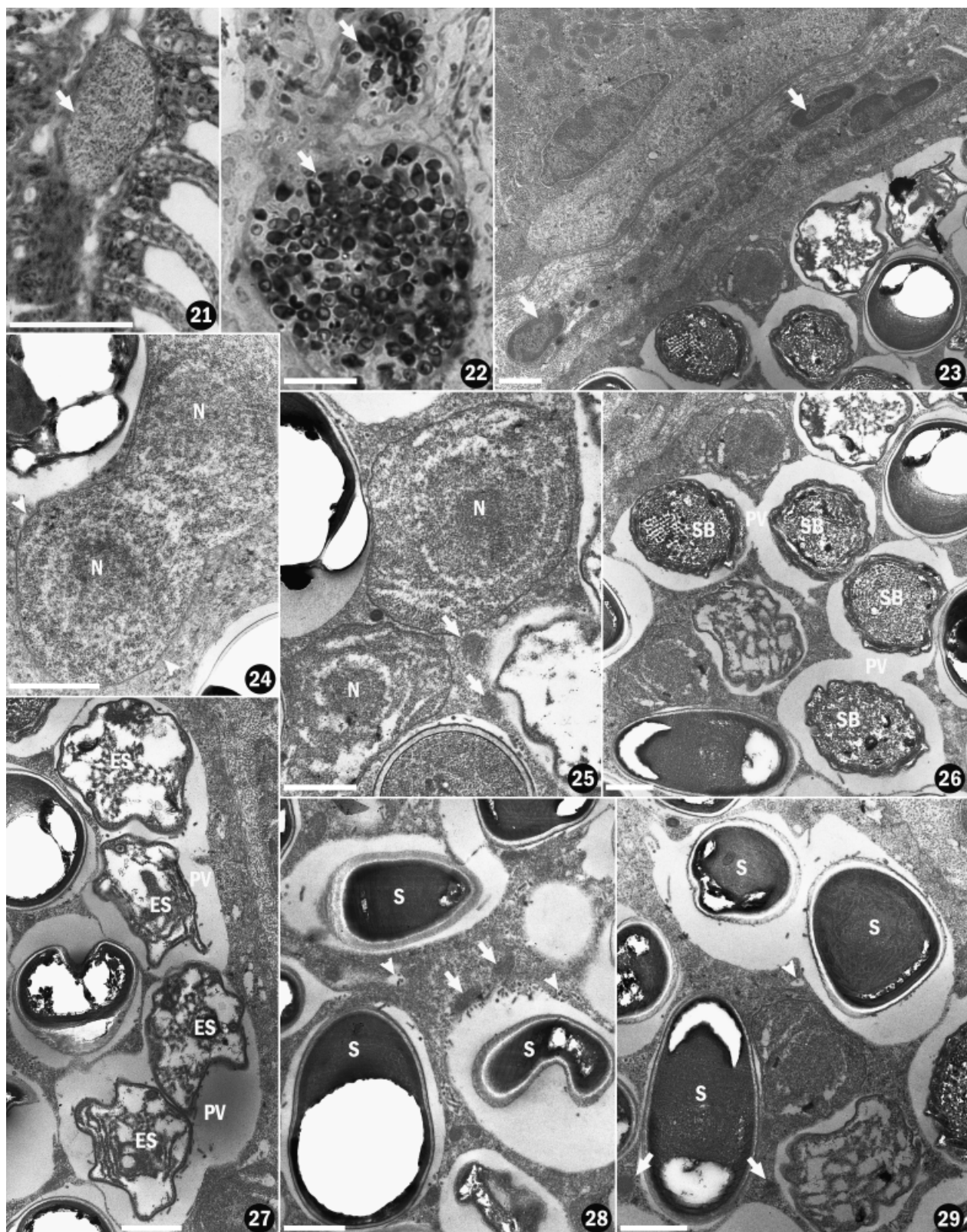
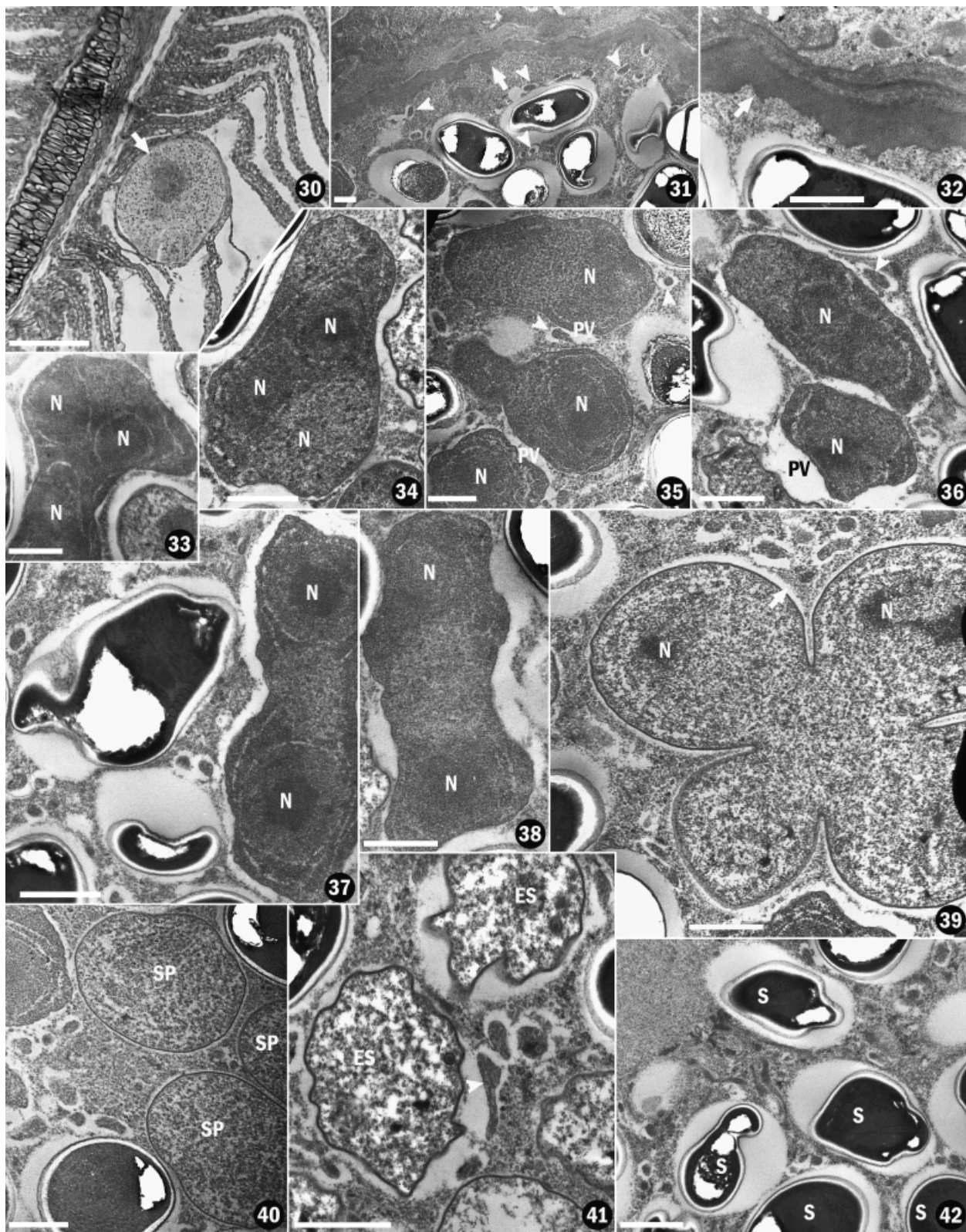


Fig. 21–29. Light (21, 22) and transmission electron micrographs (23–29) of *Loma wallae* n. sp. from walleye pollock *Theragra chalcogramma*. **21, 22.** Xenomas (arrows) in central venous sinus of gill packed densely with spores. **23.** Multilayered xenoma wall, showing smooth plasmalemma, collagenous layers, and fibroblast inclusions (arrows). **24, 25.** Meronts or merogonial plasmodia (N, nuclei) undergoing binary fission without host rough endoplasmic reticulum covering (arrowheads), and later paired with dense contents (packed ribosomes) surrounded by dark granular vesicles (arrows). **26, 27.** Products of quadri-nucleate cylindrical merogonial plasmodium: Chain of four early sporoblasts (ES) and, later, sporoblasts (SB) each developing within two closely associated parasitophorous vacuoles (PV). **28, 29.** Dark balls of amorphous material in xenoma cytoplasm (arrows) and small tubule-filled vesicles containing few tubules (arrowheads) appearing to be numerous at spore (S) surfaces. Scale bars: 100 µm (21) and 10 µm (22) and 1 µm (23–29).

host RER covering, with densely packed cytoplasmic contents undergoing binary fission (Fig. 24, 25). Cylindrical merogonial plasmodia appeared to be dividing in chains with daughters remaining together (Fig. 26, 27). Sporoblasts were within PVs

of that appeared to be of host origin, assembled in chains of four (Fig. 26, 27). Parasitophorous vacuole formation occurred before sporogony apparently by coalescence of small 60–200 nm membrane-bound vesicles and large 400–600 nm dark balls of granular



material (Fig. 28) and by coalescence of tubule-filled vesicles around later stages. Tubules were not present in PV spaces until the appearance of highly vacuolated sporoblasts (Fig. 29). Tubule-filled vesicles were small, usually arranged in a line, with few tubules per vesicle (Table 2). There were few tubule-filled vesicles associated with sporoblasts and spores (Table 2) and few tubules in PV spaces of sporoblasts and spores (Table 2). Spores were ovoid and slightly narrower at the anterior end with sub-apically situated anchoring disc with typical lamellar and vesicular polaroplasts, a singly coiled polar filament with 18.6 ± 1.8 turns (Table 2), and an exospore with fine ridges on the outer surface. Spores measured: fixed in formalin and paraffin-embedded $3.47 \pm 0.15 \mu\text{m}$ long $\times 1.93 \pm 0.09 \mu\text{m}$ wide ($n = 10$), fixed in glutaraldehyde and Spurr's resin-embedded $3.37 \pm 0.14 \mu\text{m}$ long $\times 1.81 \pm 0.05 \mu\text{m}$ wide ($n = 11$). The posterior vacuole was 1/4 to 1/3 of spore volume. There were two spores per PV, in pairs (Fig. 29).

Ecology and pathology of *Loma wallae* n. sp. “Mean” prevalence was 28.3% ($n = 145$), but as with *L. pacificodae* n. sp., the estimate depended on the method used (Table 3). Infections occurred in male and female hosts ranging in size from 12 to 48 cm. Intensity of infection ranged from one to four xenomas per gill arch to 25 xenomas per 37 primary lamellae = 0.68 xpf. Signs of host immune response were similar to those described for *L. pacificodae* n. sp., but generally less severe.

Loma kenti n. sp. (Fig. 30–42)

Morphology of *Loma kenti* n. sp. Xenomas were found primarily at the base of secondary gill lamellae arising from endothelial cells or blood vessels, throughout the primary lamellae. Xenomas were round (Fig. 30) and large (Table 2). Xenomas or spores were also found in more than half of cases in the gonads, in about half of cases in the spleen and heart, sometimes in the gallbladder, and rarely in the liver and kidney. The xenoma wall consisted of an undulating plasmalemma with $0.5\text{--}1 \mu\text{m}$ between peaks, which was covered by thick, lucent, granular, amorphous material in three layers with the innermost darkest and the outermost lightest, interspersed with collagen fibres, $1.3\text{--}3.6 \mu\text{m}$ thick (Fig. 31, 32) with 600-nm vesicle inclusions. Developmental stages and spores were intermixed with nuclei, which were always unpaired. Meronts and merogonial plasmodia had loosely packed cytoplasmic contents and a host RER covering (Fig. 46, 47) with three or more spindle plaques (Fig. 48) and with thin or up to 38-nm-thick surface glycocalyx coats. There appeared to be sporogonial plasmodia in direct contact with the xenoma cytoplasm rather than in PVs. Dark granular material in balls occurred around merogonial stages (Fig. 49). Parasitophorous vacuole formation occurred in late sporogony before or just as sporoblasts formed apparently by coalescence of tubule-filled vesicles. Tubule-filled vesicles were small, with few tubules per vesicle (Table 2). There were numerous tubule-filled vesicles associated with sporoblasts and spores (Table 2) and numerous tubules in PV spaces of sporoblasts and spores (Table 2). Spores were ovoid and slightly narrower at the anterior end with sub-apically situated anchoring disk, typical lamellar and vesicular polaroplasts, a singly coiled polar filament with 15 ± 0.7 turns (Table 2), and an exospore with fine ridges on the outer surface. Spore measurements were: fresh $4.6 (3.8\text{--}5.4) \mu\text{m}$ long $\times 2.8 (2.5\text{--}3.0) \mu\text{m}$ wide

icles, rarely with tubule-like structures visible within the granular dark material (Fig. 41) that were large (Table 2). There were no tubule-filled vesicles and no or very rarely tubules in the PV space. Spores were ovoid and slightly narrower at the anterior end with sub-apically situated anchoring disc with typical lamellar and vesicular polaroplasts, a singly coiled polar filament with 14.8 ± 0.4 turns (Table 2), and an exospore with fine ridges on the outer surface. Spore measurements were fixed in formalin and paraffin-embedded $2.97 \pm 0.13 \mu\text{m}$ long $\times 1.75 \pm 0.27 \mu\text{m}$ wide ($n = 12$), or fixed in glutaraldehyde and Spurr's resin-embedded $2.94 \pm 0.11 \mu\text{m}$ long $\times 1.52 \pm 0.05 \mu\text{m}$ wide ($n = 12$). The posterior vacuole was just under half of the spore volume. There were usually one or rarely two spores per PV (Fig. 42).

Ecology and pathology of *Loma kenti* n. sp. “Mean” prevalence was 14.4% ($n = 419$) (Table 3). Infections occurred in male and female hosts ranging in size from 12 to 14 cm. Intensity of infection ranged from one to four xenomas per gill arch to nine xenomas per 70 primary lamellae = 0.13 xpf. Signs of host immune response were rarely seen, but were similar to but less severe than those described for *L. pacificodae* n. sp.

Loma lingcodae n. sp. (Fig. 43–52)

Morphology of *Loma lingcodae* n. sp. Xenomas were found primarily in the secondary gill lamellae at tips of the primary lamellae arising from endothelial cells or the pillar system. Xenomas were round or oval (Fig. 43) and small (Table 2). Xenomas or spores were found in $\sim 90\%$ of cases in the gonads, in about half of cases in the spleen, heart, and gallbladder, and rarely in the liver and kidney. Ovaries were more heavily infected than gills in two cases, but spores were not observed inside eggs. The xenoma wall consisted of a finely undulating plasmalemma with 200–400 nm between peaks, which was covered by thick, lucent, granular, amorphous material in one layer, $0.34\text{--}0.5 \mu\text{m}$ thick (Fig. 44, 45) with 50-nm vesicle inclusions. Developmental stages and spores were intermixed with nuclei, which were always unpaired. Meronts and merogonial plasmodia had loosely packed cytoplasmic contents and a host RER covering (Fig. 46, 47) with three or more spindle plaques (Fig. 48) and with thin or up to 38-nm-thick surface glycocalyx coats. There appeared to be sporogonial plasmodia in direct contact with the xenoma cytoplasm rather than in PVs. Dark granular material in balls occurred around merogonial stages (Fig. 49). Parasitophorous vacuole formation occurred in late sporogony before or just as sporoblasts formed apparently by coalescence of tubule-filled vesicles. Tubule-filled vesicles were small, with few tubules per vesicle (Table 2). There were numerous tubule-filled vesicles associated with sporoblasts and spores (Table 2) and numerous tubules in PV spaces of sporoblasts and spores (Table 2). Spores were ovoid and slightly narrower at the anterior end with sub-apically situated anchoring disk, typical lamellar and vesicular polaroplasts, a singly coiled polar filament with 15 ± 0.7 turns (Table 2), and an exospore with fine ridges on the outer surface. Spore measurements were: fresh $4.6 (3.8\text{--}5.4) \mu\text{m}$ long $\times 2.8 (2.5\text{--}3.0) \mu\text{m}$ wide

Fig. 30–42. Light (30) and transmission electron micrographs (31–42) of *Loma kenti* n. sp. from Pacific tomcod *Microgadus proximus*. N, nuclei. 30. Xenoma (arrow) in secondary lamella of gill. 31, 32. Multilayered xenoma wall with undulating plasmalemma with a dark inner layer (arrow) and collagenous outer layers showing xenoma cytoplasm containing dark amorphous material-filled vesicles enclosed within a space (arrowheads). 33, 34. Multinucleate merogonial plasmodia densely packed with ribosomes and undergoing nuclear division with very thin surface coat (arrowhead) in direct contact xenoma cytoplasm. 35, 36. Meronts or merogonial plasmodia beginning to form parasitophorous vacuoles (PV) by the coalescence of dark material-filled vesicles at their surfaces (arrowheads) and, later, with dense cytoplasmic contents and thin surface coats in large PV spaces. 37, 38. Meronts or merogonial plasmodia dividing within a large PV space. 39. “Clover-leaf” shaped sporogonial plasmodium with thick surface coat, smooth, round shape, and reduced PV space (arrow) undergoing division by budding. 40. Three products (SP) from budding of a sporogonial plasmodium with thick surface coats, smooth, round shape, and reduced PV space. 41. Detail of dark material-filled vesicles contributing to PV space of early sporoblasts (ES) showing granular, tubule-like structures (arrowhead) within amorphous dark material. 42. Single spore (S) in each PV space. Scale bars: 100 μm (30) and 1 μm (31–42).

($n = 10$), frozen $4.8 \times (4.0\text{--}5.0) \mu\text{m}$ long $\times 2.1 \times (2.0\text{--}2.5) \mu\text{m}$ wide ($n = 30$), fixed in formalin and paraffin-embedded $2.91 \pm 0.07 \mu\text{m}$ long $\times 1.55 \pm 0.06 \mu\text{m}$ wide ($n = 17$), fixed in glutaraldehyde and Spurr's resin-embedded $3.00 \pm 0.12 \mu\text{m}$ long $\times 1.65 \pm 0.09 \mu\text{m}$ wide ($n = 10$). The posterior vacuole was less than half of the spore volume. There were four spores per PV (Fig. 50).

Ecology and pathology of *Loma lingcodae* n. sp. “Mean” prevalence was 21.4% ($n = 210$) (Table 3). Infections occurred in male and female hosts ranging in size from 45 to 82 cm, with middle-sized to larger fish more often and most heavily infected. Intensity ranged from one to four xenomas per gill arch to 65 xenomas in 28 primary lamellae = 2.3 xpfs. Signs of host immune response were rarely seen, but where observed granulomas resembled those described for *L. pacificodae* n. sp.

Loma richardi n. sp. (Fig. 53–67)

Morphology of *Loma richardi* n. sp. Xenomas were found primarily at the tips of secondary gill lamellae arising from endothelial cells or the pillar system throughout the primary lamellae (Fig. 53, 54) and were round and small (Table 2). Xenomas or spores were also found in more than half of cases in the gonads, in about half of cases in the spleen and heart, sometimes in the gallbladder, and rarely in the liver and kidney. The xenoma wall consisted of a smooth plasmalemma covered by thick, lucent, granular, amorphous material in one or two layers, $0.24 \mu\text{m}$ thick (Fig. 55–57) with 50-nm vesicle inclusions. Developmental stages and spores were intermixed with nuclei always unpaired. Merogonial plasmodia had thin, patchily distributed surface glycocalyx coats and loosely packed cytoplasmic contents in direct contact with the xenoma cytoplasm, and covered in host RER (Fig. 58). Sporonts contained concentric rings of ER cisternae (Fig. 59) and sporogonial plasmodia, sometimes dividing by binary fission, had thick surface glycocalyx coats within large PVs of host origin (Fig. 60), or sometimes at different developmental stages within a single PV space (Fig. 61, 62). Parasitophorous vacuole formation occurred before sporogony, apparently by coalescence of small, light (empty), membrane-bound vesicles (Fig. 63–65), and by coalescence of tubule-filled vesicles at later stages. Tubule-filled vesicles were large, with numerous tubules per vesicle (Table 2) and few tubule-filled vesicles associated with sporoblasts and spores (Table 2). There were numerous tubules in the PV spaces of sporoblasts and spores (Table 2). Spores were ovoid and slightly narrower at the anterior end with sub-apically situated anchoring disk, typical lamellar, and vesicular polaroplasts, a singly coiled polar filament with 13.5 ± 1.2 turns (Table 2), and an exospore with fine ridges on the outer surface. Measurements were made of spores fixed in glutaraldehyde and Spurr's resin-embedded $3.81 \pm 0.15 \mu\text{m}$ long $\times 1.93 \pm 0.15 \mu\text{m}$ wide ($n = 10$). Posterior vacuoles were almost half of the spore volume. There were two spores per PV (Fig. 66).

Ecology and pathology of *Loma richardi* n. sp. “Mean” prevalence was 13.2% ($n = 197$) (Table 3). Infections occurred in male and female hosts ranging in size from 27 to 43 cm. Intensity

of infection was generally low, at most eight xenomas per gill arch. Signs of host immune response were not seen.

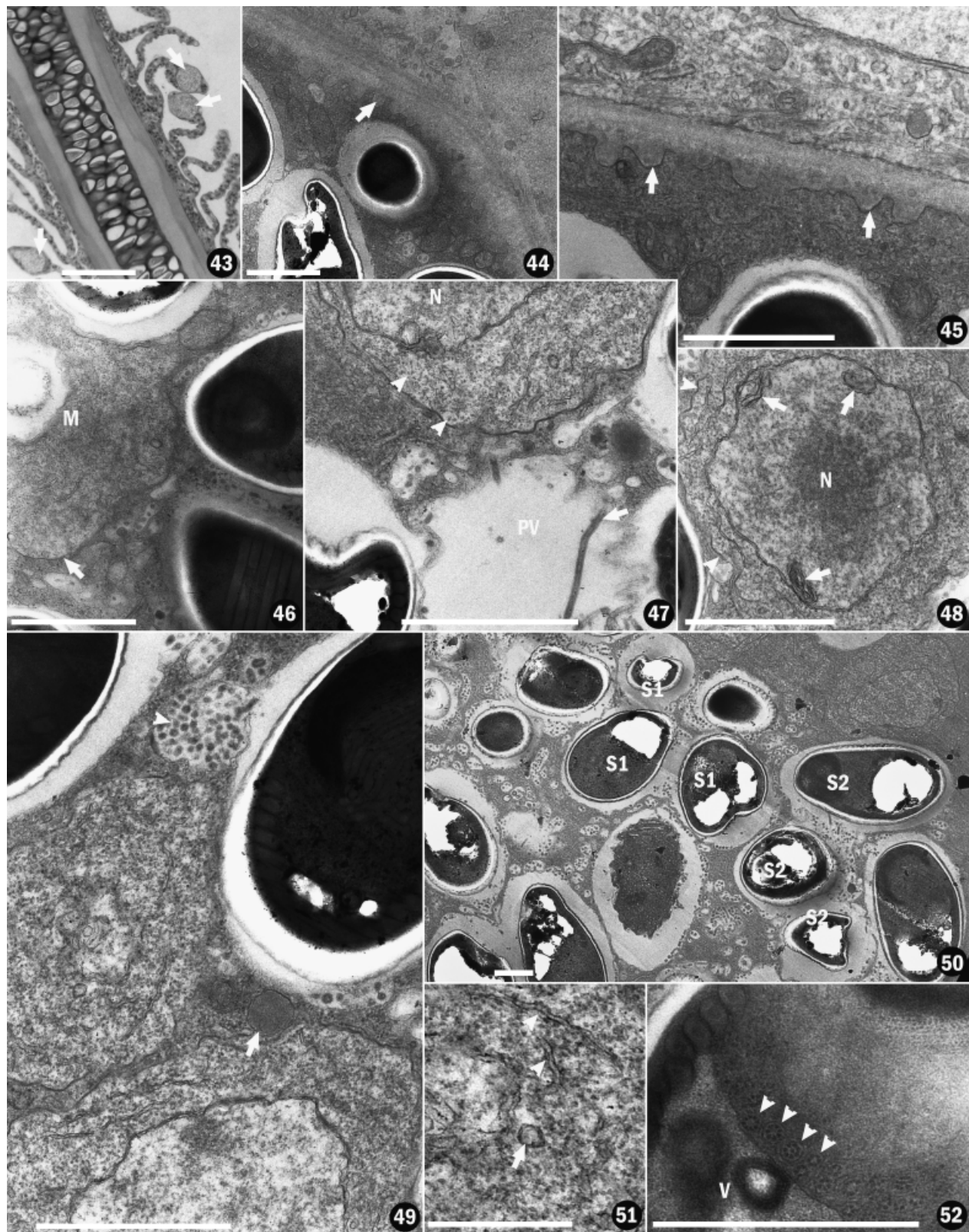
rDNA sequence characteristics. Sequences were obtained from 11 host species comprising 67 individual fishes. Each fish individual produced a *Loma* sample, designated here as an “isolate” that had one or more distinct rDNA sequences. There were seven isolates of *L. pacificodae* n. sp., four isolates of each of *L. wallae* n. sp., *L. kenti* n. sp., and *L. lingcodae* n. sp., two isolates of *L. richardi* n. sp., nine isolates of *L. morhua*, three isolates of *L. branchialis*, five isolates of *L. embiotocia*, 23 isolates of *L. salmonae*, five isolates of *Loma* sp. BRO, and one isolate of *Loma* sp. AUS. Multiple rDNA sequences in an isolate were common. For example, there were 239 unique rDNA sequences from these 67 isolates (GenBank accession numbers HQ157371–HQ157538, HM626203–HM626224). This may be due to multiple rDNA copies in a genome or multiple strains of *Loma* in the same host. Multiple rDNA sequences were observed in all *Loma* species except *Loma* sp. AUS. Divergence among sequences was greatest in species from gadid hosts and lowest in *L. salmonae* (Supporting Information Table S1). Variation included nucleotide substitutions, indels, and polymorphic differences. All species other than *Loma* sp. AUS had at least one intraspecific indel difference, many of these being parsimony informative (i.e. cases in which at least two taxa bear each state) (Supporting Information Table S2). Intra- and interspecific indels occurred in all regions (i.e. SSU, ITS, and LSU) and varied in size. Sequencing directly, without cloning, yielded double signals after indels and required FlipAnalyzer to extract sequences. Single xenoma preparations also produced such differences. Shared polymorphic differences (i.e. at least two sequences bearing each character state) or additive differences (i.e. those having all three states: two single characters and one double-signal with both single characters) occurred in all three ribosomal regions and in most species (i.e. *L. morhua*, *L. pacificodae* n. sp., *L. wallae* n. sp., *L. kenti* n. sp., *L. lingcodae* n. sp., *L. salmonae*, and *L. embiotocia*) with *L. morhua* having the most additive sites (Supporting Information Table S3). Among species in gadid hosts, 10 sites were additive (i.e. positions 157, 751, 981, 1,367, 1,393, 1,394, 1,469, 1,649, 1,717, and 1,750) and in *L. kenti* n. sp. four sites were additive (i.e. positions 1,711, 1,715, 1,717, and 1,785). Single xenomas—isolates “Gi” and “Ai” of *L. pacificodae* n. sp. and *L. morhua*, respectively, each produced two unique rDNA sequences differing by a 6-bp indel and at least six substitutions. Recombination tests using SplitsTree and LARD did not show support for recombination in any sequences.

Long rDNA amplicons were difficult to amplify for many specimens, so rDNA was often amplified and sequenced in shorter sections using internal primers (see Table 1). However, the presence of multiple unique rDNA sequences within isolates made it impossible to concatenate resulting sequences before phylogenetic analyses with confidence that the resulting fragment comprised a single strain or rDNA copy. Because one objective of the study was to examine intraspecific vs. interspecific genetic variation, a conservative approach was taken involving analysis of only non-concatenated sequences. Resulting shorter regions were as

Fig. 43–52. Light (43) and transmission electron micrographs (44–52) of *Loma lingcodae* n. sp. from lingcod *Ophiodon elongatus*. **43.** Small, round xenomas in tips of secondary lamellae of gills (arrows). **44, 45.** Xenoma wall with finely undulating plasmalemma (arrow) and light finely granular wall. **46.** Merogonial plasmodium (M) with thin surface coat (arrow) in direct contact with xenoma cytoplasm (N, nucleus) showing loosely packed ribosomes (arrowheads). A long-section of a tubule (arrow) can be seen in parasitophorous vacuole (PV). **48.** Details of meront showing three spindle plaques (arrows) within the nucleus (N) (arrowheads, meront plasmalemma). **49.** Detail of amorphous granular material in membrane-bound vesicles in xenoma cytoplasm (arrow) and tubules in a tubule-filled vesicle (arrowhead) coalescing at spore surface. **50.** Continuous PV space surrounding three spores (S1, S2). **51.** Detail of meront cytoplasm showing a double membrane-bound 75–90 nm vesicle (arrow) with slightly dark amorphous contents and nearby endoplasmic reticulum (arrowheads). **52.** Details of polyribosomes (arrowheads) lined up along posterior vacuole (V) of a spore. Scale bars: 100 μm (43), 1 μm (44–50, 52) and 0.5 μm (51).

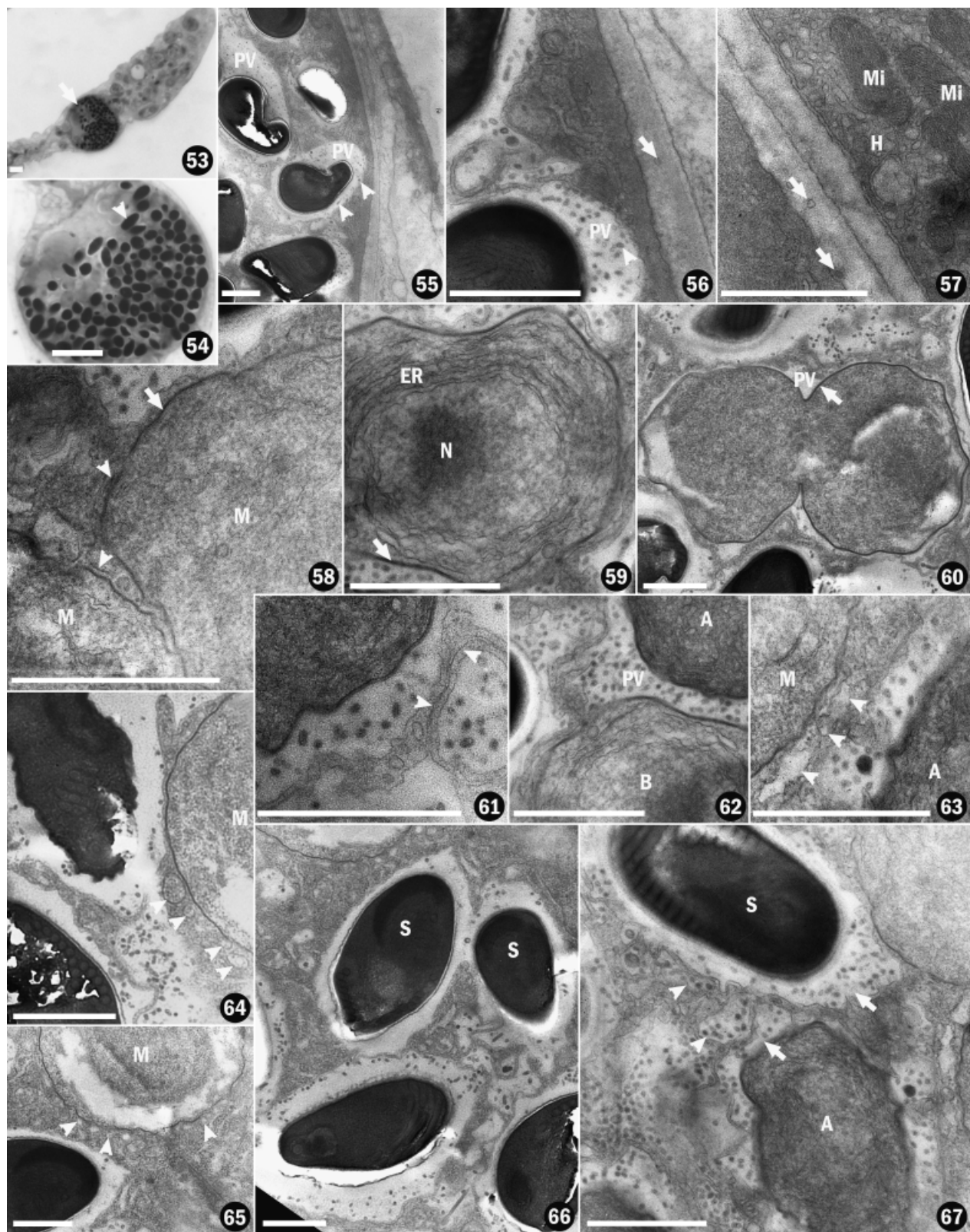
follows: region 1 (5' half of SSU) = positions 20–662, region 2 (3' half of SSU) = positions 724–1,351 and region 3 (3' end of SSU, ITS, and 5' end of LSU) = positions 1,352–1,830.

EF-1 α sequence characteristics. Sequences were obtained from two isolates of *L. pacificodae* n. sp., three isolates of *L. wallae* n. sp., two isolates each of *L. kenti* n. sp. and



L. lingcodae n. sp., three isolates of *L. morhua*, one isolate of *L. embiotocia*, 11 isolates of *L. salmonae*, and one isolate of *Loma* sp. BRO. This resulted in 19 unique sequences (GenBank accession numbers HQ157358–HQ157370, HM626225–HM6262230).

Intraspecific variation was highest in *L. morhua* and *L. pacificodae* n. sp. and lowest in *L. salmonae* and *L. kenti* n. sp. Within-



isolate sequence variation tended to be low (usually zero). Most substitutions were synonymous.

Phylogenetic relationships for rDNA region 1. For region 1, comprising 643 alignment positions, there were 16 unique rDNA sequences from eight *Loma* species. Analyses produced 35 MP trees and 15 shortest ME trees varying mostly at branch tips, and one ML tree (best-fit model F81+G) (trees not shown, but major clades and bootstrap values are shown in Fig. 68). All three types of analysis consistently produced monophyletic species-clades including all isolates of a single nominal species for *L. salmonae*, *L. kenti* n. sp., *L. wallae* n. sp., *Loma* sp. BRO, and *L. lingcodiae* n. sp. Bootstrap support from all methods was not high for isolates of *L. wallae* n. sp., which grouped either with *L. pacificodae* n. sp. or with *L. morhua* (at most 80% bootstrap support in ML, 100 replicates). Adding a gap matrix produced little change in topology or bootstrap support.

Phylogenetic relationships for rDNA region 2. For region 2, comprising 628 alignment positions, there were 37 unique sequences from 11 *Loma* species. Analyses produced six shortest ME trees, 14 ML trees (best-fit model TVM+I), and many (>900) MP trees (trees not shown, but major clades and bootstrap values are shown in Fig. 68). Most topological differences were in Clade A (*L. morhua*, *L. wallae* n. sp., and *L. pacificodae* n. sp.) and B (*L. lingcodiae* n. sp. and *L. richardi* n. sp.). Several monophyletic species-clades (i.e. *L. salmonae*, *L. embiotocia*, and *Loma* sp. BRO) were consistently obtained by all three methods with bootstrap support >80%. Three other clades were consistently observed: Clade H comprising all but one sequence from *L. branchialis*, Clade NF comprising most *L. morhua* isolates from Newfoundland, and Clade G comprising all *Loma* species from gadid hosts (i.e. *L. branchialis*, *L. morhua*, *L. pacificodae* n. sp., *L. wallae* n. sp., and *L. kenti* n. sp.), with the exception of a single isolate of *L. branchialis* (HA2), which usually, but not always, fell within this group. Isolates of *L. kenti* n. sp. grouped together in most, but not all, analyses. With a gap matrix of eight additional characters produced little change in topology and bootstrap support.

Phylogenetic relationships for rDNA region 3. For region 3, comprising 479 alignment positions, there were 72 unique sequences from 11 *Loma* species. Analyses produced one ML tree (best-fit model TVM+I+G) (Fig. 68), and many (>900) MP and ME trees, due to low resolution at branch tips. Among these trees, the most common clades were A, B, H, NF, G, and L (comprising *L. salmonae*, *Loma* sp. BRO, *L. lingcodiae* n. sp., and *L. richardi* n. sp.). Species from gadid hosts (Clade G) grouped consistently together. Consistent and high bootstrap-supported branches placed *L. salmonae* and *Loma* sp. BRO together, and isolates of *L. branchialis* (Clade H) together. Isolates of *L. kenti* n. sp. usually grouped together, but sometimes with low bootstrap support.

There were many parsimony-informative inter- and intraspecific gaps. Gap matrix data alone (21 parsimony-informative characters) without nucleotide substitutional data produced a tree (not

shown) with low resolution but a topology similar to that from nucleotide data with Clades B and G and a monophyletic species-clade for *Loma* sp. BRO. Addition of the gap matrix to the nucleotide data under ML (best-fit model GTR+I+G) produced a tree similar to that without gap data, preserving Clades G (with subclades A, NF, H) and L (with subclade B) (Fig. 68). Bootstrap support was similar or slightly higher for several nodes. Clade G formed groups suggestive of paralogous relationships among divergent rDNA copies within isolates for *L. kenti* n. sp., *L. pacificodae* n. sp., and *L. wallae* n. sp., *L. branchialis*, and *L. morhua* (see Fig. 69).

Phylogenetic analyses including polymorphic characters produced little change in topology and bootstrap support.

Phylogenetic relationships among *Loma* species for partial EF-1 α . Analyses of 19 unique sequences from eight *Loma* species (966 alignment positions) produced trees that differed slightly, depending on the analysis method. The ME tree was slightly different from MP and ML trees (best-fit model GTR+G), in that it placed one member of Clade G outside the clade. Otherwise, results were similar to those from rDNA (Fig. 70), producing Clades L (*L. salmonae* with *L. embiotocia* and *L. lingcodiae* n. sp.) with high bootstrap support, G (*Loma* species from gadid hosts) with high support, and subclade A with low support. As in the rDNA trees, *L. kenti* n. sp. was basal to Clade A. All methods placed *Loma* sp. BRO outside the group, after *Loma* sp. AUS, in a basal position after *G. plecoglossi*, with high bootstrap support.

Monophyly tests for rDNA. For region 1, four monophyly constraints were created without a gap matrix, and three constraint trees with a gap matrix (Table 6). In both cases monophyly of *L. wallae* n. sp. could not be rejected, *Loma* sp. BRO as a sister-group to *L. salmonae* could not be rejected, and *Loma* sp. from gadids grouping together could not be rejected, whereas the placement of *Loma* sp. BRO internal to the *L. salmonae* clade was rejected.

For region 2, 10 constraints were generated, both with and without addition of a gap matrix (Table 6). In both cases monophylies of *L. wallae* n. sp. or *L. pacificodae* n. sp. or *L. morhua* could not be rejected. However, the unconstrained tree in which these three species form a polyphyly could not be rejected. Placement of *L. morhua* and *L. branchialis* together as a monophyletic clade was rejected. *Loma lingcodiae* n. sp. and *L. richardi* n. sp. could not be rejected as separate clades, although the polyphyly of these species was not rejected either. *Loma* sp. BRO was rejected as a sister-group or an internal group within the *L. salmonae* clade. Because one sequence of *L. branchialis* sometimes grouped outside Clade H, two constraint trees were created to test placement of this sequence with *L. salmonae* and with *L. kenti* n. sp., and the result both with and without gaps was that these trees could not be rejected. A polyphyly of *L. kenti* n. sp. with *L. branchialis* could not be rejected.

For region 3, 10 constraint trees were generated both with and without a gap matrix (Table 6). Several results were the same,

Fig. 53–67. Light (53, 54) and transmission electron micrographs (55–67) of *Loma richardi* n. sp. from sablefish *Anoplopoma fimbria*. 53, 54. Xenoma (arrow) in secondary lamella of gill filament with densely packed mature spores (arrowhead). 55–57. Xenoma wall showing smooth plasmalemma with one or two layers of light, amorphous material and small vesicle inclusions within wall (arrows) with nearby spores within large parasitophorous vacuoles (PV) containing numerous tubules (arrowheads) and adjacent host cell (H) with oblong mitochondria (Mi). 58. Merogonial plasmodia (M) with thick surface coats (arrows) partly covered in host endoplasmic reticulum (arrowheads). 59. Sporont (N, nucleus) with thick surface coat (arrow) enclosed in a tubule-filled PV with cytoplasm containing numerous well-developed cisternae of endoplasmic reticulum (ER). 60. Dividing stage with thick surface coat (arrow) undergoing binary fission within a small PV space (PV). 61. Details of membranes surrounding tubule-filled vesicle showing extra membranes (arrowheads) that may be host endoplasmic reticulum. 62. Different stages (A and B) within the same tubule-filled PV space (PV). 63. Meront (M) with PV beginning to form at its surface by the coalescence of light vesicles (arrowheads). Tubule-filled PV space is associated with the more advanced developmental stage (A) to the lower right. 64, 65. Meronts or merogonial plasmodia (M) with light vesicles (arrowheads) accumulating at the surface. 66. Two spores (S) per PV. 67. Detail of large tubule-filled vesicles (arrowheads) and tubule-filled PV spaces (arrows) around spore (S) and earlier stage (A). Scale bars: 10 μm (54, 55) and 1 μm (56–67).

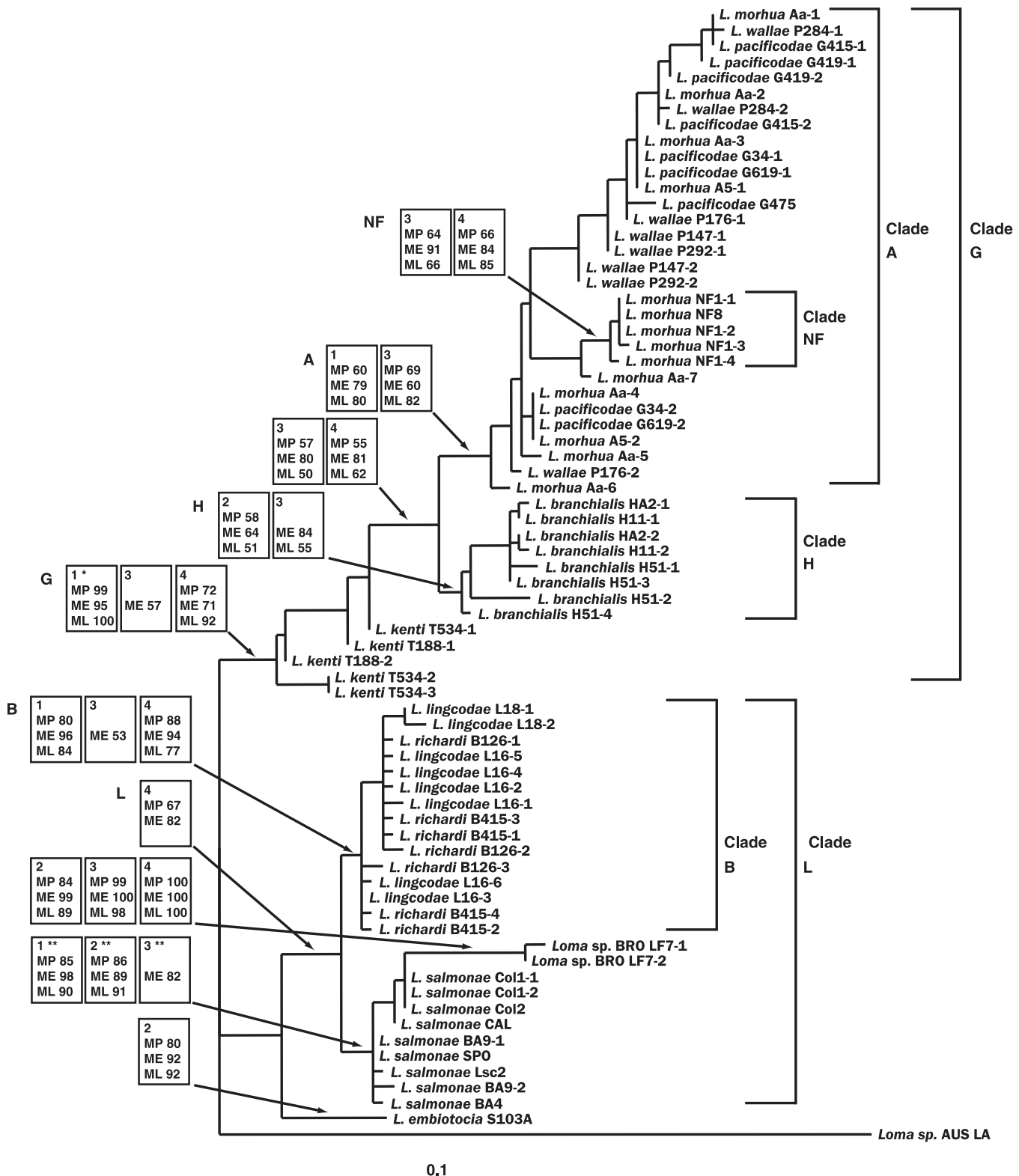


Fig. 68. Single best maximum-likelihood tree (best-fit model from Modeltest TVM+I+G) for *Loma* species including new species *L. pacificodae* n. sp., *L. wallae* n. sp., *L. kenti* n. sp., *L. lingcodae* n. sp., and *L. richardi* n. sp. estimated from 479 alignment positions of rDNA region 3 (i.e. 3' SSU, ITS, and 5' LSU) including a gap matrix of 27 additional characters, showing (in boxes) all bootstrap values above 50% for each major clade from each method and rDNA region (1, rDNA region 1, 5' half of SSU; 2, rDNA region 2, 3' half of SSU; 3, rDNA region 3 without gap matrix; 4, rDNA region 3 with addition of gap matrix). MP, maximum parsimony heuristic search with 1,000 bootstrap replicates; ME, distance logDet/paralinkar model with 1,000 bootstrap replicates; ML, maximum likelihood with best-fit model from Modeltest with 100 bootstrap replicates. Clades: NF, *Loma morhua* isolates from Newfoundland; A, monophyly of *L. morhua*, *L. pacificodae* n. sp., *L. wallae* n. sp.; H, monophyly of *L. branchialis* from haddock; G, monophyly of species from gadid hosts; B, monophyly of *L. lingcodae* n. sp. and *L. richardi* n. sp., L = *L. lingcodae* n. sp., *L. richardi* n. sp., *L. salmonae* and *Loma* sp. BRO. *These values are for *L. kenti* n. sp. Monophyly; **these values are for *L. salmonae* monophyly.

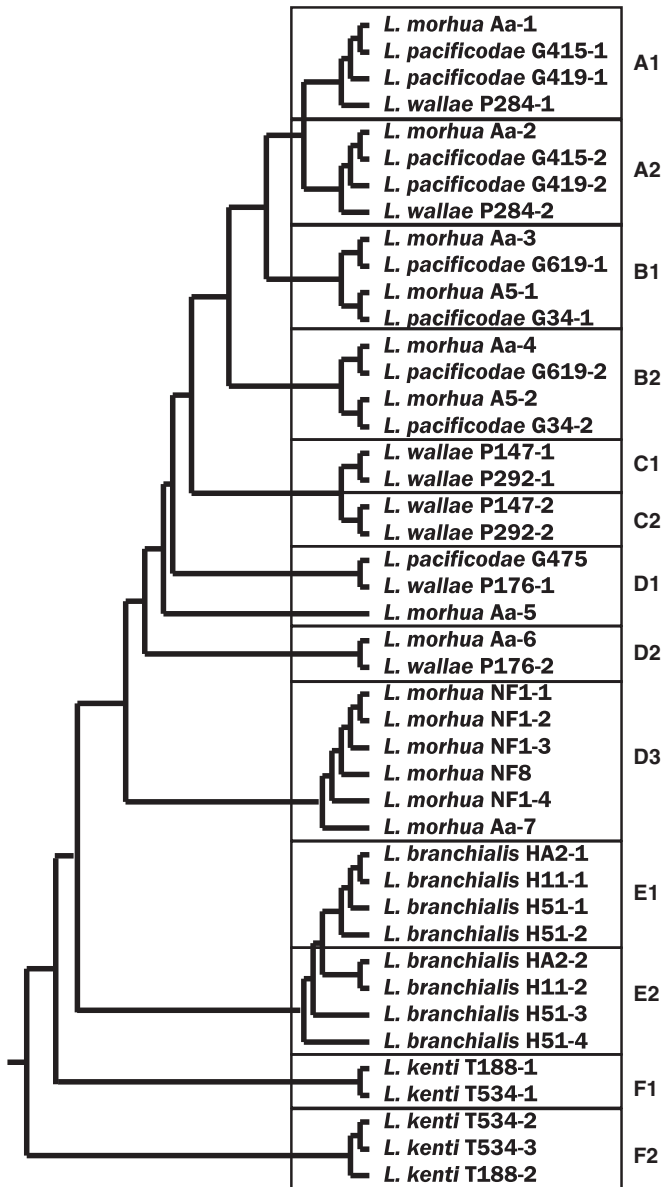


Fig. 69. Consensus 50% majority-rule maximum parsimony tree for *Loma* species including new species *L. pacificodae* n. sp., *L. wallae* n. sp., and *L. kenti* n. sp. from gadid hosts based on 479 alignment positions of rDNA (i.e. region 3, 3' SSU, ITS, and 5' LSU) including a gap matrix of 27 additional characters, showing probable orthologs in numbered boxes and close paralog sets by number (e.g. A1 is paralog of A2, B1 is paralog of B2, etc.).

regardless of whether a gap matrix was added. For example, *L. lingcodae* n. sp. and *L. richardi* n. sp. were polyphyletic in an unconstrained tree, but constraining each into monophyly could not be rejected. Separation of the *L. morhua* Clade NF to make it polyphyletic was rejected. Separation of the *L. kenti* n. sp. clade to make it paraphyletic with *L. branchialis* and others could not be rejected. Other results depended on whether a gap matrix was added. Without a gap matrix, separate monophylies for *L. wallae* n. sp., *L. pacificodae* n. sp., and *L. morhua* could not be rejected, whereas with addition of a gap matrix, these monophyletic groups were rejected. Without a gap matrix, *Loma* sp. BRO could not be rejected as a sister to *L. salmonae*, but could be rejected as an internal group in this clade, whereas with a gap matrix neither the

separation of *Loma* sp. BRO from the *L. salmonae* clade nor the placement of *Loma* sp. BRO within the *L. salmonae* clade could not be rejected.

Intraspecific indel differences affected tree topologies and were phylogenetically informative. This suggests paralogous relationships exist in Clade G. To examine whether paralogs can be grouped into orthologs by the presence or absence of two common indels, these indels were used to constrain groups of isolates. Presence or absence of the indel at positions 1,381 in the ITS or 1,622 in the LSU were used to group taxa. Without a gap matrix, grouping taxa by indels 1 and 2 was rejected, whereas with a gap matrix, such monophylies could not be rejected.

Monophyly tests for partial EF-1 α . Six constraints were generated (Table 6). Monophylies for *L. wallae* n. sp., *L. kenti* n. sp., and *L. morhua* were rejected, but monophyly of *L. pacificodae* n. sp. could not be rejected. Placement of *Loma* spp. from gadid hosts could not be rejected. However, the rejection of the unconstrained tree suggested the shortest distance tree was not the best tree when trees were evaluated using ML (lscores) under the best-fit model.

Phylogenetic position of new *Loma* species. Single reference sequences from each of the 11 *Loma* species sequenced in the present study were compared with 21 other relatives from GenBank (Fig. 71) for the SSU rDNA region alone (1,408 alignment positions) as well as for the SSU, ITS, and partial LSU rDNA region (1,936 alignment positions). Results for both regions from MP, ME, and ML were similar to that shown in Fig. 71. The 11 *Loma* species from this study formed a well-supported clade (100% bootstrap support from MP, ME, and ML) along with *Loma* sp. ‘Nil’ (an undescribed species from the fourbeard rockling *Enchelyopus cimbrius* [L.]), which clustered with *Loma* species from gadid hosts. Species relationships were similar to those obtained from rDNA regions 1, 2, and 3 (above). All analyses placed *Loma acerinae* (Jírovec, 1930) Lom & Pekkarinen, 1999 and *Loma psittaca* Casal, Matos, Teles-Grilo & Azevedo, 2009 together as a sister-clade to the *Glugea* species (Fig. 71). Groups 1 to 4 (Lom and Nilsen 2003) were well supported.

DISCUSSION

Justification for placement in genus *Loma*. The five new species had features typical of genus *Loma* Morrison & Sprague, 1981 (see Lom and Nilsen 2003): (1) xenomas of the cell-hypertrophy type in the gills, with centrally located nucleus and thick amorphous wall; (2) developmental stages and spores intermingled; (3) parasite nuclei always unpaired; (4) merogonial stages with simple plasmalemmas with thin glycocalyx coat in direct contact with xenoma cytoplasm, developing into plurinucleate plasmodia (sporogony polyploidal); (5) PV with host-derived membranes formed around developing spores; and (6) polar filaments coils arranged in one layer. Phylogenetic analyses placed the five new *Loma* species in a strongly supported clade along with the type species *L. morhua*.

Morphological justification for new *Loma* species. The five new *Loma* species differed from one another by qualitative and quantitative traits (statistically significant differences shown in Table 2) as follows. *Loma pacificodae* n. sp. was most similar to *L. wallae* n. sp., but had: more vacuolated meronts and merogonial plasmodia, presence of an additional smooth, round, thick-coated sporogonial plasmodium stage, sporogony products not associated in chains with daughter pairs remaining together, PV formation by coalescence of small, light vesicles only (not larger dark vesicles), tubules appearing in PV spaces early (rather than late), more vesicles associated with sporoblast stages, thinner xenoma walls that are less distinctly separated into layers and sometimes with interdigitated rather than smooth plasmalemma, two xenoma types,

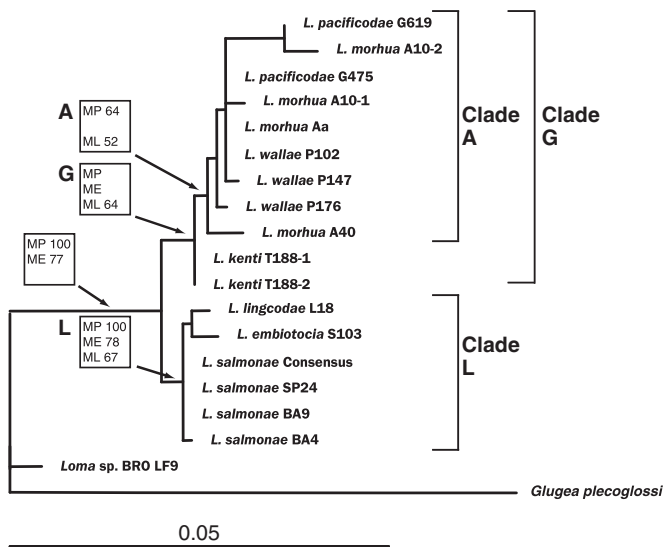


Fig. 70. Maximum-likelihood tree (best-fit model from Modeltest GTR+G) for *Loma* species including new species *L. pacificodae* n. sp., *L. wallae* n. sp., and *L. kenti* n. sp., and *L. lingcodae* n. sp. based on 966 alignment positions of elongation factor 1-alpha (*EF-1 α*), showing (in boxes) all bootstrap values above 50% for each major clade from each analysis method. MP, maximum parsimony heuristic search with 1,000 bootstrap replicates; ME, distance logDet/paralink model with 1,000 bootstrap replicates; ML, maximum likelihood with best-fit model from Modeltest with 100 bootstrap replicates. (*Glugea plecoglossi* outgroup branch has been shortened to one-sixth of original length for display purposes). Clades: A, monophyly of *L. morhua*, *L. pacificodae* n. sp., and *L. wallae* n. sp.; G, monophyly of species from gadid hosts; L, monophyly of *L. salmonae*, *L. lingcodae* n. sp., and *L. embiotocia*.

one being larger and the other smaller than that of *L. wallae* n. sp., absence of large balls of dark granular material contributing to the PV space, wider spores (resin), and slightly longer (resin and histological sections) and wider (histological sections) spores but with low statistical support ($P > 0.1$). *Loma pacificodae* n. sp. differed from *L. kenti* n. sp. in having later PV formation, more vacuolated meronts, different vesicles contributing to PV space formation, these vesicles being smaller and more numerous, presence of tubules in vesicles and PV spaces, larger spores, and more polar filament turns. *Loma pacificodae* n. sp. was somewhat similar to *L. lingcodae* n. sp., but could be distinguished by having: xenomas located in the central venous sinus of the primary lamellae rather than at the tips of the secondary lamellae, xenomas of different cell type, shape, and size with different wall features, with presence of small (empty) vesicles that coalesce to form PV spaces, PV space formation earlier with respect to surface coat formation, presence of sporogonial plasmodia, two (rather than four) spores per PV space, larger spores, more polar filament turns, and fewer tubules per vesicle. *Loma pacificodae* n. sp. differed from *L. richardi* n. sp. in having: larger xenomas differing in ways similar for *L. lingcodae* n. sp., as well as smaller vesicles and fewer tubules per vesicle, more vesicles per sporoblast, fewer tubules per sporoblast and spore PV, shorter spores (resin), and more polar filament turns.

Loma wallae n. sp. could be distinguished from *L. kenti* n. sp. by many of the same features shared with *L. pacificodae* n. sp.: for example, by having later PV formation, smaller and more numerous vesicles contributing to PV space formation, presence of tubules in vesicles and PV spaces, longer spores, and more polar filament turns. *Loma wallae* n. sp. differed from *L. lingcodae* n. sp. in features shared with *L. pacificodae* n. sp.: for example by having xenomas in the central venous sinus rather than at tips of the secondary lamella, xenomas of different cell type, shape, and size and with a smooth

rather than undulating wall, presence of small (empty) vesicles that coalesce to form PV spaces, PV space formation earlier with respect to surface coat formation, two (rather than four) spores per PV space, fewer vesicles per sporoblast, longer spores, and more polar filament turns. *Loma wallae* n. sp. and *L. richardi* n. sp. differed in ways similar to that described for *L. pacificodae* n. sp., such as larger xenoma of different shape, cell type, location, and wall features, as well as smaller vesicles and fewer tubules per vesicle, fewer tubules per sporoblast and spore PV (resin), and more polar filament turns.

Loma kenti n. sp. was similar in spore size to *L. lingcodae* n. sp., but could be distinguished by having earlier PV formation while its merogonial surface coat is thin, dark material-filled rather than tubule-filled vesicles contributing to PV space formation, no tubules in either vesicles or PV spaces, larger vesicle size, and fewer vesicles per sporoblast and spore. *Loma kenti* n. sp. could be distinguished from *L. richardi* n. sp. in many of the same ways described for the species from lingcod: for example, in having earlier PV formation, dark material-filled rather than tubule-filled vesicles, no tubules, as well as by having shorter spores.

Loma lingcodae n. sp. was most similar to *L. richardi* n. sp. but could be distinguished by having an undulating single-layered rather than smooth double-layered xenoma wall, slightly larger xenomas (not statistically significant), uninucleate meronts, later formation of PV spaces after the surface coat had greatly thickened, no sporogonial stages surrounded by PV spaces, no large dark vesicles contributing to the PV space formation, four spores per PV space rather than two, smaller vesicles and fewer tubules per vesicle, more vesicles per sporoblast, fewer tubules per spore PV, and smaller (resin) and shorter (converted) spores.

New *Loma* species differed from previously described *Loma* species as follows (and see Table 4). The spores of *L. wallae* n. sp., *L. kenti* n. sp., and *L. lingcodae* n. sp. were smaller than those from *L. morhua* and *L. branchialis*. Spores of *L. pacificodae* n. sp. were shorter than those of *L. morhua* and smaller than those of *L. branchialis*, but the latter was not statistically significant. Spores of *L. richardi* n. sp. were narrower than those of *L. morhua*. *Loma pacificodae* n. sp. also differed from *L. morhua* and *L. branchialis* in being located in the Pacific rather than Atlantic Ocean in Pacific cod rather than Atlantic cod or haddock, and in having less dense material filling PV spaces, smaller spores (accounting for fixation shrinkage), less invaginated walls, smaller xenomas, spores in pairs rather than singly, and an absence of double-sized, binucleate spores (Morrison and Marryatt 1986; Morrison and Sprague 1981a, b). *Loma pacificodae* n. sp. differed from *L. salmonae* and *L. embiotocia* in host order, and polar filaments appearing later during sporogony, fewer merogonial nuclei, smaller xenomas, fibroblast connective tissue rather than endothelial cells forming xenomas, more polar filament turns, and a marine rather than freshwater or anadromous life history compared with *L. salmonae*, and tubules arising in empty vesicles of host origin rather than from within a granular substance of host origin, and larger spores compared with *L. embiotocia*. *Loma pacificodae* n. sp. differed from *Loma fontinalis* Morrison & Sprague, 1983, *Loma mugili* Ovcharenko, Sarabev, Wita & Czaplińska, 2000, *Loma diplodae* Bekhti & Bouix, 1985, *Loma* sp. of Bekhti 1984, and *Loma trichiuri* Sandeep & Kalvati, 1985 in being in a gadid host in the Pacific Ocean, and in having sporogonic stages and sporoblasts within a PV space. It also had smaller xenomas compared with *L. fontinalis* and *L. mugili*, located primarily in the central venous sinus rather than secondary lamellae of the gills and sporogonic vacuole formation by coalescence of vesicles from the host rather than by blistering or delamination of material from the parasite compared with *L. diplodae*. Xenomas were in the central venous sinus or base of the secondary lamellae rather than in the adductor muscle of the gills and with a wall not covered in reticulated meshwork compared with *Loma*

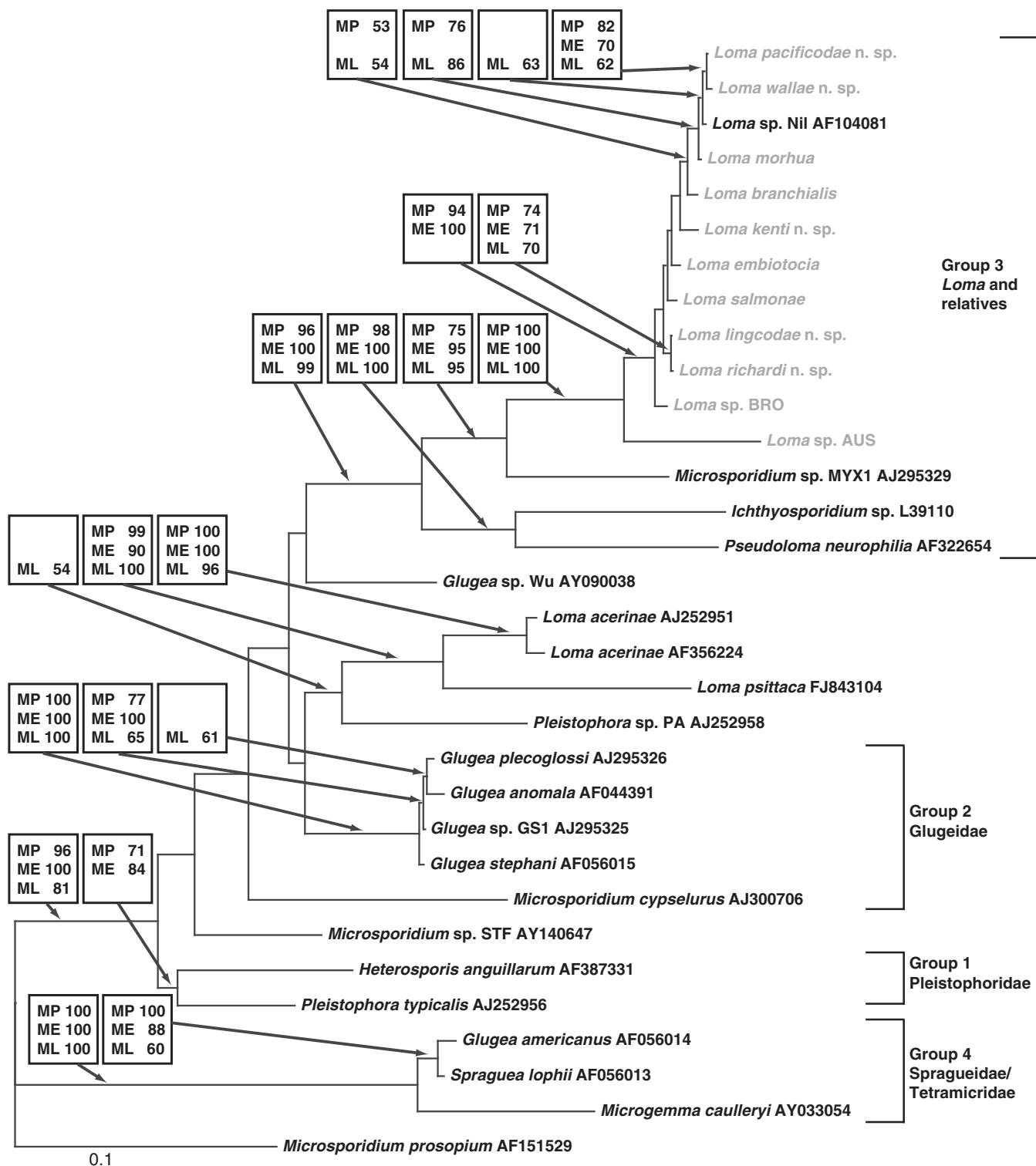


Fig. 71. Maximum-likelihood (ML) tree generated from 1,936 alignment positions of rDNA from the SSU, ITS, and partial LSU for all available *Loma* species and close relatives showing strong support for “true” *Loma* species clustered around the type species *Loma morhua* and for Groups 1 to 4 (from Lom and Nilsen 2003). *Loma acerinae* and *Loma psittaca* clearly do not cluster with true *Loma* species. Concatenated sequences for *Loma* species (present study, in gray) were created from the most common nucleotide at each position from all isolates. Boxes show bootstrap values above 50% from each method (MP, maximum parsimony heuristic search with 1,000 bootstrap replicates; ME, minimum distance logDet/paralink model with 1,000 bootstrap replicates, ML best-fit model from Modeltest GTR+I+G with 100 bootstrap replicates). GenBank accession numbers are shown next to species names.

Table 4. Summary of host, site, locality, spore, xenoma, and polar filament features for described *Loma* species (measurements in μm).

Species and reference	Host	Site	Locality	Spore			Polar filament turns	Xenoma size
				Shape	L	W		
<i>L. branchialis</i> (Morrison and Sprague 1981a, b) ^a	<i>Melanogrammus aeglefinus</i>	Gill filaments	Marine (Boreo-Arctic)	Ellipsoidal/ovoid	4.2	2.0	16–17	50–150
<i>L. salmoniae</i> (Putz et al. 1965)	<i>Oncorhynchus mykiss</i>	Gill filaments	Freshwater (Several countries)	Pyriform/ellipsoidal	3.74–4.4	2.2–2.3	12–14	14–17
<i>L. fontinalis</i> (Morrison & Sprague, 1983)	<i>Sauvulus fontinalis</i>	Gill lamellae	Freshwater (Canada)	Pyriform/ellipsoidal	3.7	2.3	12–14	500
<i>L. dimorpha</i> (Loubès et al. 1984)	<i>Gobius niger</i> (and others)	Digestive tract connective tissue	Marine (France and Spain)	Ovoid/ellipsoidal	4.5	1.8–2.0	13–15	100–300
<i>L. diplodae</i> (Bekhti and Bouix 1985)	<i>Diplodus sargus</i>	Gill filament vessels	Marine (France)	Ovoid	4.17	2.22	17–18	150
<i>L. trichiuri</i> (Sandep and Kalavati 1985)	<i>Trichurus savala</i>	Gill filaments	Marine (India)	Pyriform	3.0	2.0	250–500	
<i>L. camerounensis</i> (Fomene et al. 1992)	<i>Oerochromis niloticus</i>	Esophagus to intestine	Freshwater (Cameroon)	Ovoid	3.96	2.16	11–12	340
<i>L. boopst</i> (Faye et al. 1995)	<i>Boops boops</i>	Liver and digestive tract	Marine (Senegal)	Ovoid/elongate	3.74–4.8	2.4–2.4	12–14	16–18
<i>L. embiotocia</i> (Shaw et al. 1997)	<i>Cymatogaster aggregata</i>	Gills	Marine (Canada)	Ovoid	4.8	2.6	14–18	1,000–1,500
<i>L. acerinae</i> (Lom and Pekkarinen 1999)	<i>Gymnocephalus cernuus</i>	Intestine wall	Freshwater (Czech Republic)	Ellipsoidal	4.64	2.19	11–23	60–160
<i>L. mugilii</i> (Ovcharenko et al. 2000)	<i>Mugil soyus</i>	Gills	Marine (Sea of Azov)	Ovoid/elongate	3.48	2.18	14–15	300
<i>L. myrophis</i> (Azevedo and Matos 2002)	<i>Myrophis playphyneus</i>	Gut subepithelial tissue	Freshwater (Brazil)	Ellipsoidal	3.45	1.71	13–14	350
<i>L. psittaca</i> (Casal et al. 2009)	<i>Colomesus psittacus</i>	Intestinal wall	Freshwater (Brazil)	Ovoid	4.2	2.8	11–12	310
<i>L. pacificodae</i> n. sp. (present study)	<i>Gadus macrocephalus</i>	Gill central venous sinus	Marine (British Columbia)	Ovoid	5.5–3.48	3.0–1.95	16–22	47.3–120.1
<i>L. wallae</i> n. sp. (present study)	<i>Theragra chalcogramma</i>	Gill central venous sinus	Marine (British Columbia)	Ovoid	3.37	1.81	16–21	82.9
<i>L. kentii</i> n. sp. (present study)	<i>Microgadus proximus</i>	Gill secondary lamellae	Marine (British Columbia)	Ovoid	2.94	1.52	14–16	142.3
<i>L. lingcodae</i> n. sp. (present study)	<i>Ophiodon elongatus</i>	Gill secondary lamellae	Marine (British Columbia)	Ovoid	4.63	2.8–1.65	14–16	37.4
<i>L. richardi</i> n. sp. (present study)	<i>Anoplopoma fimbria</i>	Gill secondary lamellae	Marine (British Columbia)	Ovoid	3.81	1.93	11–15	33.1

^aFurther detail on *Loma branchialis* and *Loma morhua* is shown in Table 5. Spores were either resin embedded or fresh (indicated by boldface).

sp. of Bekhti; and ovoid rather than pyriform spores, fewer merogonial nuclei and thinner wall compared with *L. trichiuri*. *Loma pacificodae* n. sp. differed from *L. acerinae*, *L. psittaca*, *Loma dimorpha* Loubès, Maurand, Gasc, De Buron & Barral, 1984, *Loma boopst* Faye, Toguebaye & Bouix, 1995, *Loma myrophis* Azevedo & Matos, 2002, and *L. camerounensis* in having xenomas primarily in the gills rather than the gut and occurring in gadid rather than non-gadid hosts in the Pacific Ocean rather than other localities. It also differed from and *L. diplodae* and all the latter, except *L. acerinae* and *L. psittaca*, in having membranes of host origin (i.e. true PV) around sporogonic stages formed by coalescence of vesicles rather than parasite-derived sporophorous vesicles resulting from blistering or delamination of material from the sporont surface.

Loma wallae n. sp. differed from described *Loma* species as listed for *L. pacificodae* n. sp. except that it had only one xenoma type and smooth rather than highly invaginated xenoma wall compared with *L. branchialis* and *L. morhua*. The same was true of *L. kentii* n. sp., except that compared with others it had empty or dark material-filled rather than tubule-filled vesicles contributing to PV spaces and earlier appearance of PV spaces. It also had a simple xenoma wall compared with *L. branchialis* and *L. morhua*, and compared with *L. salmonae* and *L. embiotocia*, it was more similar in polar filament turns (Shaw et al. 1997).

Loma lingcodae n. sp. and *L. richardi* n. sp. differed from described species much like *L. pacificodae* n. sp. except that they were similar to *L. salmonae* and *L. embiotocia* in polar filament turn number and in forming xenomas from epithelial cells, but *L. lingcodae* n. sp. differed in having four spores per PV, smaller spores, and a finely undulating wall. Compared with *L. branchialis* and *L. morhua*, these species had one xenoma type, a Scorpaeniformes rather than Gadiformes host, fewer polar filament turns, a simple, smooth wall with amorphous light contents, and *L. lingcodae* n. sp. had four rather than two spores per PV.

Phylogenetic justification for new *Loma* species. Molecular data varied in support for these five new *Loma* species, depending on the DNA region and method of analysis. For example, though most analyses supported species designation for *L. kentii* n. sp. and two separate species-clades (A and B), most did not resolve the two pairs of new species (*L. pacificodae* n. sp., *L. wallae* n. sp., and *L. lingcodae* n. sp. and *L. richardi* n. sp.) in each of these clades. However, statistical tests generally could not reject monophyly for these four species. For example, *L. pacificodae* n. sp. and *L. wallae* n. sp., which failed to resolve into species monophylies for all but one DNA region (i.e. the 5' SSU region resolved *L. wallae* n. sp. with low bootstrap support), AU tests usually did not reject species monophylies, except for the SSU/ITS/LSU region with gap matrix added and for the *EF-1 α* gene for *L. wallae* n. sp. The first of these results can be explained by paralogs, particularly because evidence showed at least two gaps (indels) clearly segregated as paralogs. Elongation factor 1-alpha results may also be explained by paralogs or pseudogenes and the higher intraspecific divergence in Clade G. The presence of two sequences from one isolate of *L. morhua* suggests this gene may be multicopy, at least in this clade. Similarly, analyses could not resolve *L. lingcodae* n. sp. and *L. richardi* n. sp., yet AU tests did not reject monophyly. Paralogs could also potentially be responsible for this low resolution. For *L. kentii* n. sp., some analyses produced a paraphyletic clade, yet AU tests could not reject monophyly or paraphyly. Only for *EF-1 α* did AU tests reject monophyly in favour of paraphyly for *L. kentii* n. sp.; however, this clade may be affected by paralogs (as above).

Most species definitions expect all members of a species to form a monophyletic clade, whereas a polyphyly or polytomy suggests insufficient evidence for species; however, there are many explanations for low genetic divergence among good

morphospecies, as was observed here. In *Loma* and other microsporidia, explanations may include unusually conserved genes (Cho et al. 1995; Corradi et al. 2007; Katinka et al. 2001), insufficient length of gene examined to observe evolutionary divergence (e.g. recent speciation) (Cheney, Lafranchi-tristem, and Canning 2000; Lom and Nilsen 2003; Nilsen and Chen 2001), gene reticulation due to paralogs (Bell, Aoki, and Yokoyama 2001, Cheney et al. 2001; O'Mahony, Tay, and Paxton 2007; Tay, O'Mahony, and Paxton 2005; and the present study), and species hybridization or reticulate speciation.

Ecology, pathology, and development. *Loma pacificodae* n. sp. and *L. wallae* n. sp. were found in approximately one-third of their respective hosts and the least prevalent species, *L. richardi* n. sp., still occurred in more than 10% of hosts, suggesting these are widespread pathogens. Host susceptibilities, movements, parasite virulence, or life cycles could all contribute to prevalence differences between species; however, geographic differences in prevalence in *L. pacificodae* n. sp. suggest host susceptibility is important, as has been suggested for *L. salmonae* (Shaw et al. 2000a; Shaw, Kent, and Adamson 2000a, 2001). Pathogenesis in these species was similar to that observed for other *Loma* species (Becker and Speare 2007; Kent and Speare 2005; Lovy et al. 2007), suggesting hosts may be able to develop resistance to reinfection. Site of infection seemed to show a relationship with prevalence and host response (e.g. xenomas in the central venous sinus showed more host response and were at higher prevalence than those in the secondary lamellae).

The presence of all of these *Loma* species in the gonads raises the possibility that they may transmit vertically, as has been suggested for *L. salmonae* and *L. morhua* (Docker et al. 1997a; Morrison 1983) and other microsporidia (Dunn, Terry, and Smith 2001; Smith 2009). Vertical transmission in *Loma* species could have implications for virulence as predicted by models and experimental studies (Agnew and Koella 1997; Dunn and Smith 2001; Lipsitch, Siller, and Nowak 1996).

Developmental sequences appeared to correlate with xenoma size. For example, spores nearly filled the volume of mature xenomas, suggesting development proceeds to a species-characteristic climax, at which point xenomas are full of spores and have a characteristic (diagnostic) size. This is in contrast to previous assumptions that division is asynchronous (Lom and Pekkarinen 1999). Interestingly, species with significantly larger xenomas (e.g. *L. kenti* n. sp. and *L. pacificodae* n. sp.) also displayed an additional developmental stage (i.e. a sporogonial “rounded up” stage). This relationship should be examined further as it may be diagnostically useful.

Phylogenetic analyses of all available *Loma* species along with outgroup taxa further support the findings of (Casal et al. 2009; Lom and Nilsen 2003) that the genus is polyphyletic with outliers *L. aceriniae* and *L. psittaca* not belonging in genus *Loma*. Key features that separate all “true” *Loma* species from these outliers, which may therefore be considered diagnostic for *Loma* are: (1) site of infection (gills, rather than gut), (2) developmental sequence (largely determinate, rather than asynchronous), and (3) episporoblastic space (not filled with dense granular material, rather than filled with this material).

Justification for validity of *L. branchialis* and *L. morhua*.

Recent molecular data have raised questions about the validity of the type species (Brown and Kent 2002). When genus *Loma* was erected for type species *L. morhua* Morrison & Sprague, 1981 from Atlantic cod, an earlier described species from haddock *Melanogrammus aeglefinus* (L.), originally *Nosema branchiale* Nemeczek, 1911 and later *Glugea branchiale* (Nemeczek, 1911) Lom & Laird, 1976, was transferred to *L. branchialis* (Morrison and Marryatt 1986; Morrison and Sprague 1981a, b). Subsequent authors considered differences between these two species (spore- and xenoma size and wall features) to be inadequate, making them

synonymous and designating the earlier described species *L. branchialis* as the type (Canning and Lom 1986). However, both molecular and morphological data in the present study support the designation of *L. branchialis* and *L. morhua* as separate, valid species. For example, rDNA consistently placed them in separate clades, and AU tests always rejected their monophyly. Morphological data in the present study also appear to support the designation of *L. branchialis* and *L. morhua* as separate species. For example, spores from *L. morhua* in Atlantic cod were significantly larger than those from *L. branchialis* in haddock (student *t*-test *P*-value 0.007 from ethanol-fixed spores), and the two had qualitatively different xenomas. Finding two statistically distinct spore sizes in two sympatric hosts is considered a significant indicator of species-level difference (Lom 2002; Lom and Pekkarinen 1999). Most previous studies support the present study, showing spores from haddock are smaller (Table 5). For example, when shrinkage was taken into account, spores from haddock in New Brunswick, Canada (Lom and Laird 1976) were smaller than those from Atlantic cod in the Gulf of St. Lawrence, Canada (Fanham, Porter, and Richardson 1941). Still, comparison with type specimens for *L. branchialis* and *L. morhua* is necessary. The type description of *L. morhua* shows the opposite pattern from that found in the present study for the same hosts from the same location (Morrison and Sprague 1981a, b) (Table 5); however, no variance around the mean was provided. Spores of the type specimen for *L. branchialis* in northeastern North America or Russia (Nemeczek 1911) were still larger than those observed in the present study, accounting for shrinkage; however, range, variance, and mean were not given, making statistical comparison impossible. Nevertheless, the present molecular and morphological data together with most historical comparisons support two separate species. Thus, *L. morhua* should be hereafter recognized again as a valid species. It would therefore be the type species as originally proposed by Morrison and Sprague (1981a).

***Loma salmonae* variant SV.** Material designated *Loma* sp. BRO here was alternately named “*L. salmonae* SV” (Sánchez et al. 2001a). Yet our results showed that these were clearly separate species. Thus, “SV” is not a variant of *L. salmonae*. The source of this material may explain the results. Spores of *Loma* sp. BRO came from laboratory experiments to transmit *L. salmonae* from *Oncorhynchus* spp. in British Columbia to laboratory-held brook trout in Prince Edward Island. Resulting spores were different in biology from *L. salmonae* (Sánchez et al. 2001a, b; Speare and Daley 2003). Thus, it appears brook trout used in the trial may have carried an undetected or cryptic infection of a separate *Loma* species. It is unclear whether this could be *L. fontinalis*, a *Loma* species native to brook trout near the source of fish in this study (Cobequid hatchery, Nova Scotia, Canada), because neither detailed morphological analysis nor DNA sequences are available for these specimens.

Co-evolution and phylogeography. In the present study, as in previous reviews of microsporidia, the host was an important indicator of species (Baker, Vossbrinck, Becnel & Andreadis 1998; Lom and Nilsen 2003; Smith 2009; Vossbrinck and Debrunner-Vossbrinck 2005) and parasites grouped by host as opposed to geography. For example, the tree topology for five *Loma* species in gadid hosts was congruent to that of the hosts produced from mitochondrial cytochrome *b* and cytochrome oxidase I genes (Carr et al. 1999). Carr et al. (1999) could not resolve these hosts (i.e. Pacific cod, Atlantic cod, and walleye pollock), suggesting recent speciation or possibly species hybridization. A molecular clock (Bermingham, McCafferty, and Martin 1997) suggesting three independent Pacific basin invasions by *Microgadus*, *Gadus*, and *Theragra* species during the re-opening of the Bering Strait 3.0–3.5 million years ago (mya) (Carr et al. 1999), together with the congruence between host and parasite phylogenies suggests *L. kenti* n. sp. diverged earliest from the Atlantic basin predeces-

Table 5. Comparison of *L. branchialis* and *L. morhua* with converted spore sizes estimated from shrinkage factors for each fixation method.

Author	Host	Locality	Fixation	Xenoma size (mm)	Spore size (μm)	Converted size range of spores this study (μm)	
						<i>L. morhua</i> (All)	<i>L. branchialis</i> (Had)
Nemeczek (1911)	Had	America/Russia	Fz	0.2–0.5, 1	L W	6.3 3.5	5.16–5.24 2.89–3.11
Bazilakova (1932)	Had and (Atl)	Barents Sea	—	—	—	—	4.85–5.09 2.83–2.97
Dogiel (1936)	Kild	Barents Sea	Fz	—	L	5–6	4.85–5.09
Fantham, Porter, and Richardson (1941)	Atl	Gulf of St. Lawrence	Fsh	—	L	5.7–6.6	5.54–5.86
Shulman and Shulman-Albova (1953)	Green	White Sea	Fm	—	W	3.5–4.2	3.06–3.22
Kabata (1959)	Atl	Southern Iceland	Fm	0.5–1.2	W	4.3–5.1	N/A
Lom and Laird (1976)	Had	New Brunswick	Fsh	1.2	L W	4.9 2.4	N/A
Morrison and Sprague (1981a) ^a	Atl	Halifax, NS	R	0.05–0.15	L W	4.2 2.0	5.83–6.13 3.13–3.35
Morrison and Sprague (1981b) ^a	Had	Halifax, NS	R	—	L W	4.4 2.1	3.06–3.22 3.15–3.40
This study	Atl	Halifax, NS	Et	—	L W	4.32 2.43	1.65–1.77 1.65–1.77
This study	Had	Halifax, NS	Et	—	L W	4.13 2.35	N/A

^aOriginally named *L. morhua*. Conversion estimates fresh spore dimensions.
Had, haddock, *Melanogrammus aeglefinus*; Atl, Atlantic cod, *Gadus morhua*; Kild, Kildin cod, *G. morhua kildinensis*; Green, Greenland cod, *Gadus agac*; Fz, frozen; Fsh, fresh; Fm, formalin; R, resin; Et, ethanol; (All), authors reported haddock were more often infected.

sors (12 mya), followed by *L. branchialis* and its host (7–8 mya), *L. pacificodae* n. sp. and host (3.5 mya), and then *L. wallae* n. sp. and host (3.0 mya). Assuming an equal SSU rDNA evolutionary rate among close relatives, for *Loma* species this would be 0.1458% per million years (based on 1.958 bp change per 1,344 bp length) and the rate of speciation can be estimated. For example, close species *L. salmonae* and *L. embiotocia*, which have been demonstrated to be non-transmissible to reciprocal hosts may have diverged about 5.1 mya (based on 0.741% SSU difference). By comparison, divergence within these species ranged from 100,000 to 1 mya, compared with 2.6 mya (0.38% SSU divergence) for *L. lingcodae* n. sp., a species that was also demonstrated to be non-transmissible to sympatric *Loma* hosts (*Oncorhynchus* spp.) (Shaw et al. 2000c; Shaw, pers. commun.).

Paralogs and reticulation. Evidence suggested that low resolution in Clades A and B may be caused by (1) recent speciation (discussed above); (2) rDNA paralogs grouping into copy-based rather than species-based clusters, and/or (3) species hybridization or rDNA recombination. Indeed, paralogs seemed common (e.g. see relationships among seven rDNA sequences from isolate Aa) and clearly occurred in two isolates Gi and Ai, each producing two unique rDNA sequences, and each derived from a single xenoma which presumably resulted from vegetative divisions of a single spore (with a single genome). Diverged rDNA paralogs have been shown by direct evidence from a single spore by others (O'Mahony et al. 2007; Tay et al. 2005). As well, additive shared polymorphisms, which are considered to be evidence of recombination across species (e.g. in mussels of *Mytilus* spp. and corals of *Madracis* spp., Diekmann et al. 2001), were common in the present study. For example, in Clade G 10 sites were additive and in *L. kenti* n. sp. four sites were additive. For one additive site in *L. kenti* n. sp. (i.e. position 1,717 of the rDNA cistron in the 5' region of the LSU) character states matching both *L. salmonae* and *L. embiotocia* suggest species hybridization with geographic (rather than phylogenetic) sister-species. Furthermore, indels, which were common in these species, may point to past hybridization (e.g. as for simian immunodeficiency virus, see Cheynier et al. 2001). While indels in *Loma* may not accumulate at the high rate they do in a retrovirus, they would still occur by a double strand DNA break followed by a repair mistake. Indeed, repair apparatus function may be especially reduced due to parasitic reduction of the microsporidian genome (Katinka et al. 2001; Williams 2009). Species hybridization or rDNA recombination would seem to require a sexual cycle; however, which at present is not known for *Loma* species, this have unpaired nuclei in all stages (Lom 2002). In summary, these possibilities should act to warn future researchers of the importance of sequencing multiple isolates and clones for studies of closely related microsporidia.

Together, the present study provided morphological and DNA data to support the description of five new species of *Loma* in five Pacific fishes.

TAXONOMIC SUMMARY

Phylum Microsporidia Balbiani, 1882
Class Haplophasea Sprague, Becnel & Hazard, 1992
Order Glugeida Issi, 1986
Family Glugeidae Thélohan, 1892
Genus *Loma* Morrison & Sprague, 1981

Loma pacificodae n. sp.

Diagnosis. Xenoma of cell-hypertrophy form with enlarged, branched, but not divided host nuclei, of two shapes: elongate ($120.1 \pm 14.1 \mu\text{m}$, $n = 43$); and round ($47.3 \pm 15.0 \mu\text{m}$, $n = 15$). Xenoma wall smooth or interdigitated plasmalemma covered by

Table 6. Monophyly test statistics for *Loma* species generated by CONSEL showing *P*-values for unconstrained and monophyly-constrained trees for three ribosomal DNA regions with and without addition of a gap matrix and for elongation factor 1-alpha (*EF-1 α*).

Constraint	Test results (<i>P</i> -values)					Conclusion
	AU	KH	SH	WKh	WSH	
rDNA region 1 without gap matrix						
1 Unconstrained	0.522	0.395	0.796	0.395	0.793	Do not reject
2 <i>L. wallae</i> n. sp. monophyly	0.645	0.605	0.787	0.605	0.802	Do not reject
3 <i>Loma</i> sp. BRO sister to <i>L. salmoniae</i>	0.040	0.235	0.576	0.154	0.469	Do not reject
4 <i>Loma</i> sp. BRO internal to <i>L. salmoniae</i>	2e-074	0.004	0.005	0.001	0.003	Reject
5 <i>Loma</i> sp. from gadids monophyly	0.298	0.288	0.546	0.288	0.596	Do not reject
rDNA region 1 with gap matrix added						
6 Unconstrained	0.424	0.345	0.762	0.345	0.701	Do not reject
7 <i>L. wallae</i> n. sp. monophyly	0.409	0.413	0.608	0.413	0.597	Do not reject
8 <i>Loma</i> sp. BRO sister to <i>L. salmoniae</i>	0.599	0.655	0.913	0.587	0.917	Do not reject
9 <i>Loma</i> sp. BRO internal to <i>L. salmoniae</i>	1e-010	0.001	0.007	0.001	0.001	Reject
rDNA region 2 without gap matrix						
1 Unconstrained	0.821	0.511	0.967	0.511	0.967	Do not reject
2 <i>L. wallae</i> n. sp. monophyly	0.736	0.381	0.966	0.381	0.966	Do not reject
3 <i>L. pacificodae</i> n. sp. monophyly	0.751	0.489	0.981	0.489	0.981	Do not reject
4 <i>L. morhua</i> monophyly	0.068	0.153	0.836	0.153	0.545	Do not reject
5 <i>L. branchialis</i> with <i>L. morhua</i>	0.005	0.034	0.169	0.034	0.078	Reject
6 <i>L. lingcodae</i> and <i>L. richardi</i> separate	0.070	0.141	0.404	0.132	0.313	Do not reject
7 <i>Loma</i> sp. BRO sister to <i>L. salmoniae</i>	0.006	0.076	0.229	0.035	0.083	Reject
8 <i>Loma</i> sp. BRO internal to <i>L. salmoniae</i>	1e-005	0.010	0.055	0.010	0.020	Reject
9 <i>L. branchialis</i> "HA2" with <i>L. salmoniae</i>	0.387	0.376	0.869	0.376	0.867	Do not reject
10 <i>L. branchialis</i> "HA2" with <i>L. kenti</i> n. sp.	0.735	0.381	0.966	0.381	0.966	Do not reject
11 <i>L. kenti</i> polyphyletic with <i>L. branchialis</i>	0.821	0.511	0.967	0.511	0.967	Do not reject
rDNA region 2 with gap matrix added						
12 Unconstrained	0.836	0	0.995	0	0.995	Do not reject
13 <i>L. wallae</i> n. sp. monophyly	0.836	0.304	0.989	0.304	0.989	Do not reject
14 <i>L. pacificodae</i> n. sp. monophyly	0.244	0.216	0.886	0.216	0.695	Do not reject
15 <i>L. morhua</i> monophyly	0.040	0.103	0.626	0.103	0.383	Do not reject
16 <i>L. branchialis</i> with <i>L. morhua</i>	0.004	0.056	0.181	0.056	0.128	Reject
17 <i>L. lingcodae</i> and <i>L. richardi</i> separate	0.069	0.104	0.529	0.104	0.247	Do not reject
18 <i>Loma</i> sp. BRO sister to <i>L. salmoniae</i>	0.010	0.076	0.267	0.043	0.106	Reject
19 <i>Loma</i> sp. BRO internal to <i>L. salmoniae</i>	7e-005	0.012	0.064	0.012	0.025	Reject
20 <i>L. branchialis</i> "HA2" with <i>L. salmoniae</i>	0.425	0.376	0.843	0.376	0.830	Do not reject
21 <i>L. branchialis</i> "HA2" with <i>L. kenti</i> n. sp.	0.836	0	0.995	0	0.995	Do not reject
22 <i>L. kenti</i> polyphyletic with <i>L. branchialis</i>	0.107	0.147	0.685	0.147	0.410	Do not reject
rDNA region 3 without gap matrix						
1 Unconstrained	0.039	0.110	0.813	0.110	0.556	Do not reject
2 <i>L. wallae</i> n. sp. monophyly	0.761	0.612	0.956	0.612	0.959	Do not reject
3 <i>L. pacificodae</i> n. sp. monophyly	0.542	0.388	0.935	0.388	0.919	Do not reject
4 <i>L. morhua</i> monophyly	0.112	0.088	0.824	0.088	0.404	Do not reject
5 <i>Loma</i> sp. BRO sister to <i>L. salmoniae</i>	0.168	0.147	0.738	0.147	0.588	Do not reject
6 <i>L. richardi</i> and <i>L. lingcodae</i> separate	0.039	0.110	0.813	0.110	0.556	Do not reject
7 <i>L. kenti</i> n. sp. paraphyletic	0.187	0.170	0.783	0.170	0.620	Do not reject
8 <i>L. morhua</i> "NF" polyphyletic	0.003	0.011	0.039	0.011	0.032	Reject
9 <i>Loma</i> sp. BRO internal to <i>L. salmoniae</i>	0.003	0.042	0.305	0.042	0.136	Reject
10 <i>Loma</i> spp. grouped by indel 1 (ITS)	0.007	0.023	0.168	0.023	0.056	Reject
11 <i>Loma</i> spp. grouped by indel 2 (LSU)	7e-005	0.010	0.021	0.004	0.008	Reject
rDNA region 3 with gap matrix added						
12 Unconstrained	0.510	0.244	0.941	0.244	0.890	Do not reject
13 <i>L. wallae</i> n. sp. monophyly	0.004	0.013	0.086	0.013	0.071	Reject
14 <i>L. pacificodae</i> n. sp. monophyly	7e-012	0.012	0.050	0.002	0.011	Reject
15 <i>L. morhua</i> monophyly	0.010	0.018	0.088	0.018	0.087	Reject
16 <i>Loma</i> sp. BRO and <i>L. salmonse</i> separate	0.016	0.017	0.248	0.017	0.072	Do not reject
17 <i>L. richardi</i> and <i>L. lingcodae</i> separate	0.374	0.310	0.657	0.310	0.678	Do not reject
18 <i>L. kenti</i> n. sp. paraphyletic	0.796	0.756	0.980	0.690	0.985	Do not reject
19 <i>L. morhua</i> "NF" polyphyletic	3e-092	3e-004	0.004	3e-004	0.001	Reject
20 <i>Loma</i> sp. BRO internal to <i>L. salmoniae</i>	0.076	0.101	0.661	0.101	0.441	Do not reject
21 <i>Loma</i> spp. grouped by indel 1 (ITS)	0.113	0.080	0.450	0.080	0.317	Do not reject
22 <i>Loma</i> spp. grouped by indel 2 (LSU)	0.018	0.019	0.159	0.019	0.071	Do not reject
Partial <i>EF-1α</i> gene						
1 Unconstrained	0.005	0.049	0.087	0.049	0.094	Reject
2 <i>L. morhua</i> monophyly	4e-004	0.060	0.087	0.052	0.134	Reject
3 <i>L. wallae</i> n. sp. monophyly	0.005	0.081	0.424	0.081	0.199	Reject
4 <i>L. pacificodae</i> n. sp. monophyly	0.103	0.221	0.517	0.230	0.527	Do not reject
5 <i>L. kenti</i> n. sp. monophyly	0.005	0.081	0.424	0.081	0.199	Reject
6 <i>Loma</i> spp. from gadids monophyly	0.720	0.668	0.906	0.668	0.918	Do not reject
7 <i>L. morhua</i> , <i>L. pacificodae</i> and <i>L. wallae</i>	0.470	0.332	0.687	0.332	0.713	Do not reject

Conclusions are based on AU test with rejection at the *P*-value of $\alpha = 0.01$.

"monophyly," all isolates form a strictly monophyletic clade; "sister to," forming sister monophyletic clades; "internal to," forming a nested clade within a monophyletic clade of both groups; "with," forming a monophyletic clade of all isolates but polyphyletic with respect to species; separate," = forming separate monophylies.

thick electron-lucent, granular material in one layer ($1.5\text{--}2.0\,\mu\text{m}$ thick) mixed with collagen fibres with fibroblast inclusions. Collagenous material in middle of xenomas. Developmental stages and spores intermixed, nuclei always unpaired. Uninucleate meronts with thin surface glycocalyx coat in direct contact with host cytoplasm, undergoing binary fission within a host RER covering; highly vacuolated merogonial plasmodia; oblong, rounded, sporogonial plasmodia with smooth, thick glycocalyx coat enclosed within PV of host origin. Parasitophorous vacuole formation before sporogony by coalescence of light $60\text{--}200\,\text{nm}$ membrane-bound vesicles and, later, tubule-filled vesicles. Tubules present in PV spaces before sporogony. Tubule-filled vesicles small ($0.203 \pm 0.033\,\mu\text{m}$, $n = 16$) with few tubules per vesicle (3 ± 0.6 , $n = 33$). Numerous tubule-filled vesicles in xenoma cytoplasm associated with sporoblast (8.0 ± 2.0 , $n = 7$) and spore (3.8 ± 1.2 , $n = 10$). Numerous tubules in PV spaces of sporoblast (19.3 ± 14.0 , $n = 4$) and spore (9 ± 3.1 , $n = 12$). Spores ovoid and slightly narrower at anterior end with sub-apically situated anchoring disc, lamellar and vesicular polaroplasts, singly coiled polar filament, and exospore with fine ridges. Spores: fresh 5.5 ($4.8\text{--}6.0\,\mu\text{m}$) \times 3.0 ($2.7\text{--}3.2\,\mu\text{m}$) ($n = 10$), frozen 4.6 ($4.0\text{--}5.5\,\mu\text{m}$) \times 2.5 ($2.0\text{--}3.0\,\mu\text{m}$) ($n = 30$), paraffin embedded $3.58 \pm 0.15 \times 1.94 \pm 0.15\,\mu\text{m}$ ($n = 10$), Spurr's resin embedded $3.48 \pm 0.23 \times 1.95 \pm 0.12\,\mu\text{m}$ ($n = 12$). Polar filament turns 17.9 ± 0.9 (range $16\text{--}22$) ($n = 14$). Posterior vacuole small (one-fourth of spore). Two spores per PV.

Type host. Pacific cod, *Gadus macrocephalus* Tilesius, 1810.

Type locality. Queen Charlotte Sound Canada ($50^\circ 52'N$, $127^\circ 21'W$).

Site of infection. Primarily central venous sinus of gills in fibroblast connective tissue or lymph vessel, or at base of secondary lamellae in cells of the pillar system. Secondarily in gonads, spleen, heart, gallbladder, liver, and kidney.

Prevalence. 32.6% ($n = 227$).

Type material. Hapantotype deposited in the Canadian Museum of Nature Parasite Collection, Catalogue number CMNPA 2010-0003.

Gene sequence. GenBank Accession (HQ157410–HQ157433, HQ157362–HQ157363).

Etymology. The specific name reflects that of the type host (Pacific cod), and is feminine gender, in accordance with the International Code of Zoological Nomenclature.

Loma wallae n. sp.

Diagnosis. Xenoma of cell-hypertrophy form with enlarged, branched, but not divided host nuclei, round shape often septate $82.9 \pm 16.9\,\mu\text{m}$ ($n = 25$) wide. Xenoma wall a smooth plasmalemma covered by thick electron-lucent, granular material in three layers with collagenous fibres and fibroblast inclusions, $2.5\,\mu\text{m}$ thick. Developmental stages and spores intermixed, nuclei always unpaired. Uninucleate meronts with thin glycocalyx coat without host RER covering with densely packed cytoplasmic contents undergoing binary fission or cylindrical merogonial plasmodia dividing in chains, daughters remaining together; sporoblasts within PVs of host origin in chains of four, in closely associated pairs closely. Parasitophorous vacuole formation before sporogony by coalescence of small, light $60\text{--}200\,\text{nm}$ membrane-bound vesicles and large $400\text{--}600\,\text{nm}$ dark balls of granular material and, later, tubule-filled vesicles. Tubules not present in PV spaces until appearance of highly vacuolated sporoblasts. Tubule-filled vesicles small, usually in a line ($0.260 \pm 0.046\,\mu\text{m}$, $n = 10$), with few tubules per vesicle (4.0 ± 1.0 , $n = 23$). Few tubule-filled vesicles in xenoma cytoplasm associated with sporoblast (1.9 ± 0.8 , $n = 9$) and spore (3.6 ± 1.7 , $n = 14$). Few tubules in PV spaces of sporoblast (8.0 ± 3.8 , $n = 7$) and spore (5.9 ± 2.5 , $n = 10$). Spores ovoid and slightly narrower at anterior end with sub-ap-

cally situated anchoring disc, lamellar and vesicular polaroplasts, singly coiled polar filament and exospore with fine ridges. Spores: paraffin-embedded $3.47 \pm 0.15 \times 1.93 \pm 0.09\,\mu\text{m}$ ($n = 10$), Spurr's resin-embedded $3.37 \pm 0.14 \times 1.81 \pm 0.05\,\mu\text{m}$ ($n = 11$). Polar filament turns 18.6 ± 1.8 (range $16\text{--}21$) ($n = 5$). Posterior vacuole small (one-fourth–one-third of spore). Two spores per PV in pairs.

Type host. Walleye pollock (= Alaska pollock), *Theragra chalcogramma* (Pallas, 1814).

Type locality. Barkley Sound, Vancouver Island, Canada ($48^\circ 46'N$, $125^\circ 29'W$).

Site of infection. Central venous sinus of gills, in fibroblast connective tissue. Secondarily in gonads, spleen, heart, liver, kidney, and especially gallbladder.

Prevalence. 28.3% ($n = 145$).

Type material. Hapantotype deposited in the Canadian Museum of Nature Parasite Collection, Catalogue number CMNPA 2010-0005.

Gene sequence. GenBank Accession (HQ157434–HQ157469, HQ157364–HQ157366).

Etymology. The specific name reflects that of the type host (walleye pollock), and is feminine gender, in accordance with the International Code of Zoological Nomenclature.

Loma kenti n. sp.

Diagnosis. Xenoma of cell-hypertrophy form with enlarged, branched, but not divided host nuclei, round and $142.3 \pm 24.0\,\mu\text{m}$ ($n = 8$) wide. Xenoma wall an undulating plasmalemma ($0.5\text{--}1\,\mu\text{m}$ between peaks) covered by thick electron-lucent, granular material in three layers interspersed with collagen fibres, $1.3\text{--}3.6\,\mu\text{m}$ thick. Vesicle inclusions $600\,\text{nm}$. Developmental stages and spores intermixed, nuclei always unpaired. Plurinucleate merogonial plasmodia (nuclei clustered) with densely packed cytoplasmic contents, with thin, patchily distributed surface glycocalyx coats with beginnings of PV formation or with fully formed large PV spaces of host origin, usually associated in pairs, and not covered in host RER; oblong or round, sporogonial plasmodia with smooth, thick glycocalyx coats dividing by multiple fission (a “clover-leaf”). Parasitophorous vacuole formation at merogonial stages by coalescence or emptying of vesicles containing dark balls of granular material within a vacuolar space. Dark material-filled vesicles large ($0.715 \pm 0.212\,\mu\text{m}$, $n = 15$). No tubule-filled vesicles. No tubules in PV space. Spores ovoid and slightly narrower at anterior end with sub-apically situated anchoring disc, lamellar and vesicular polaroplasts, singly coiled polar filament, and exospore with fine ridges. Spores: paraffin-embedded $2.97 \pm 0.13 \times 1.75 \pm 0.27\,\mu\text{m}$ ($n = 12$), Spurr's resin-embedded $2.94 \pm 0.11 \times 1.52 \pm 0.05\,\mu\text{m}$ ($n = 12$). Polar filament turns 14.8 ± 0.4 (range $14\text{--}16$) ($n = 12$). Posterior vacuole large (<1/2 of spore). One or rarely two spores per PV.

Type host. Pacific tomcod, *Microgadus proximus* (Girard, 1854).

Type locality. Barkley Sound, Vancouver Island, Canada ($48^\circ 46'N$, $125^\circ 20'W$).

Site of infection. Base of secondary lamellae and blood vessels of gills, in endothelial cells. Secondarily in gonads, spleen, heart, gallbladder, liver, and kidney.

Prevalence. 14.4% ($n = 419$).

Type material. Hapantotype deposited in the Canadian Museum of Nature Parasite Collection, Catalogue number CMNPA 2010-0001.

Gene sequence. GenBank Accession (HQ157470–HQ157487, HQ157367–HQ157368).

Etymology. Named after one of the fathers of protozoology, William Saville-Kent (1845–1905).

***Loma lingcodae* n. sp.**

Diagnosis. Xenoma of cell-hypertrophy form with enlarged, branched, but not divided host nuclei, round or oval and $37.4 \pm 3.9 \mu\text{m}$ ($n = 56$) wide. Xenoma wall a finely undulating plasmalemma (200–400 nm between peaks) covered by thick electron-lucent, granular material in one layer, $0.34\text{--}0.5 \mu\text{m}$ thick. Vesicle inclusions 50 nm. Developmental stages and spores intermixed, nuclei always unpaired. Meronts and merogonial plasmodia with loosely packed cytoplasmic contents and host RER covering and with three or more spindle plaques, with glycocalyx coats (up to 38 nm) in direct contact with host cytoplasm. Dark granular material in balls accumulated around merogonial stages. Parasitophorous vacuole formation in late sporogony before or as sporoblasts form, by coalescence of tubule-filled vesicles. Tubule-filled vesicles small ($0.277 \pm 0.027 \mu\text{m}$, $n = 19$), with few tubules per vesicle (6.1 ± 0.7 , $n = 28$). Numerous tubule-filled vesicles in the host cytoplasm associated with sporoblast (7.0 ± 1.3 , $n = 9$) and spore (4.8 ± 1.0 , $n = 10$). Numerous tubules in PV spaces of sporoblast (17 ± 6.4 , $n = 7$) and spore (11.8 ± 2.9 , $n = 23$). Spores ovoid and slightly narrower at anterior end with sub-apically situated anchoring disk, lamellar and vesicular polaroplasts, singly coiled polar filament, and exospore with fine ridges. Spores: fresh 4.6 ($3.8\text{--}5.4 \mu\text{m} \times 2.8$ ($2.5\text{--}3.0 \mu\text{m}$)) ($n = 10$), frozen 4.8 ($4.0\text{--}5.0 \mu\text{m} \times 2.1$ ($2.0\text{--}2.5 \mu\text{m}$)) ($n = 30$), paraffin-embedded $2.91 \pm 0.07 \times 1.55 \pm 0.06 \mu\text{m}$ ($n = 17$), Spurr's resin-embedded $3.00 \pm 0.12 \times 1.65 \pm 0.09 \mu\text{m}$ ($n = 10$). Polar filament turns 15 ± 0.7 (range 14–16) ($n = 6$). Posterior vacuole large (<1/2 of spore). Four spores per PV.

Type host. Lingcod, *Ophiodon elongatus* Girard, 1854.

Type locality. West Coast of Vancouver Island, Canada ($49^{\circ}34'N$, $127^{\circ}12'W$).

Site of infection. Secondary lamellae of gills, primarily at tips of primary filaments, in endothelial cells or pillar system. Secondary in spleen, heart, liver, gallbladder, kidney, and especially gonads.

Prevalence. 21.4% ($n = 210$).

Type material. Hapantotype deposited in the Canadian Museum of Nature Parasite Collection, Catalogue number CMNPA 2010-0004.

Gene sequence. GenBank Accession (HQ157501–HQ157524, HQ157369).

Etymology. The specific name reflects that of the type host (lingcod), and is feminine gender, in accordance with the International Code of Zoological Nomenclature.

***Loma richardi* n. sp.**

Diagnosis. Xenoma of cell-hypertrophy form with enlarged, branched, but not divided host nuclei, round and $33.1 \pm 1.4 \mu\text{m}$ ($n = 5$) wide. Xenoma wall a smooth plasmalemma covered by thick electron-lucent, granular material in one or two layers, $0.24 \mu\text{m}$ thick. Vesicle inclusions 50 nm. Developmental stages and spores intermixed, nuclei always unpaired. Merogonial plasmodia with thin, patchily distributed surface glycocalyx coats and loosely packed cytoplasmic contents in direct contact with host cytoplasm, and covered in host RER; sporonts with concentric rings of ER cisternae and sporogonial plasmodia with thick surface glycocalyx coats within large PVs of host origin, sometimes dividing by binary fission, sometimes at different developmental stages within a single PV. Parasitophorous vacuole formation early, before sporogony by coalescence of small, light, membrane-bound vesicles, and later, tubule-filled vesicles. Tubule-filled vesicles large ($0.658 \pm 0.133 \mu\text{m}$, $n = 16$), with numerous tubules per vesicle (15.6 ± 4.7 , $n = 20$). Few tubule-filled vesicles associated with sporoblast (3.5 ± 1.3 , $n = 4$) and spore (2.5 ± 1.0 , $n = 8$). Many tubules in PV space of sporoblast (90.3 ± 40.6 , $n = 4$) and spore (52 ± 7.2 , $n = 16$). Spores ovoid

and slightly narrower at anterior end with sub-apically situated anchoring disk, lamellar and vesicular polaroplasts, singly coiled polar filament, and exospore with fine ridges. Spores: Spurr's resin-embedded $3.81 \pm 0.15 \times 1.93 \pm 0.15 \mu\text{m}$ ($n = 10$). Polar filament turns 13.5 ± 1.2 (range 11–15) ($n = 6$). Posterior vacuole large (<1/2 of spore). Two spores per PV.

Type host. Sablefish (= blackcod), *Anoplopoma fimbria* (Pallas, 1814).

Type locality. West Coast of Vancouver Island, Canada ($48^{\circ}54'N$, $126^{\circ}11'W$).

Site of infection. Tips of secondary lamellae of gills throughout primary lamellae, in endothelial cells or pillar system. Secondary in gonads, spleen, heart, gallbladder, liver, and kidney.

Prevalence. 13.2% ($n = 197$).

Type material. Hapantotype deposited in the Canadian Museum of Nature Parasite Collection, Catalogue number CMNPA 2010-0004.

Gene sequence. GenBank Accession (HQ157488–HQ157500).

Etymology. Named after the late mathematician and evolutionary biology hobbyist, Dr. Richard L. W. Brown.

ACKNOWLEDGEMENTS

We sincerely thank staff at the Pacific Biological Station in Nanaimo, Canada and R. W. Shaw for assistance with collection of material. We also thank R. Adlard and J. G. Sánchez-Martínez for providing material from Australia and Prince Edward Island, respectively. We thank S. Johnson for help with collection of Atlantic cod and haddock heads. We are grateful to technicians at the BioImaging Facility (UBC) for help with ultrathin sectioning and TEM. We thank the laboratory of P. J. Keeling for assistance with cloning. This work was supported by Natural Sciences and Engineering Research Council of Canada Strategic grant 58073 to M.L.A.

LITERATURE CITED

- Agnew, P. & Koella, J. C. 1997. Virulence, parasite mode of transmission, and host fluctuating asymmetry. *Proc. R. Soc. Ser. B Biol. Sci.*, **264**: 9–15.
- Akaike, H. 1974. A new look at the statistical model identification. *IEEE Trans. Automat. Control*, **19**:716–723.
- Azevedo, C. & Matos, E. 2002. Fine structure of a new species, *Loma myrophis* (Phylum Microsporidia), parasite of the Amazonian fish *Myrophis platycephalus* (Teleostei, Ophichthidae). *Eur. J. Protistol.*, **37**:445–452.
- Baker, M. D., Vossbrinck, C. R., Beclen, J. J. & Andreadis, T. G. 1998. Phylogeny of *Amblyospora* (Microsporidia: Amblyosporidae) and related genera based on small subunit ribosomal DNA data: a possible example of host-parasite cospeciation. *J. Invert. Pathol.*, **71**:199–206.
- Baker, M. D., Vossbrinck, C. R., Didier, E. S., Maddox, J. V. & Shadduck, J. A. 1995. Small subunit ribosomal DNA phylogeny of various microsporidia with emphasis on AIDS-related forms. *J. Eukaryot. Microbiol.*, **42**:564–570.
- Bazilakova, A. 1932. Beiträge zur Parasitologie der Murman'schen Fische. Sbornik Nauchno-Promyslovikh Rabot na Murman. In: Mittelman, S. Y. (ed.), Narkomsnab SSR Tsentral'nya. Institut Rybnogo Khozyaistva, Moskva, Leningrad, Russia. p. 136–153.
- Becker, J. A. & Speare, D. J. 2007. Transmission of the microsporidian gill parasite, *Loma salmonae*. *Anim. Health Res. Rev.*, **8**:59–68.
- Bekhti, M. 1984. Étude comparative des espèces des microsporidies parasites des poissons téléostéens du littoral languedocien. Rapport D. E. A., Université des Sciences et Techniques du Languedoc, Montpellier, p. 32.
- Bekhti, M. & Bouix, G. 1985. *Loma salmonae* (Putz, Hoffman et Dunbar, 1965) et *Loma diplodae* n. sp., microsporidies parasites de branchies de poissons téléostéens: implantation et données ultrastructurales. *Protistologica*, **21**:47–59.

- Bell, A. S., Aoki, T. & Yokoyama, H. 2001. Phylogenetic relationships among microsporidia based on rDNA sequence data, with particular reference to fish-infecting *Microsporidium* Balbiani 1884 species. *J. Eukaryot. Microbiol.*, **48**:258–265.
- Bermingham, E., McCafferty, S. S. & Martin, A. P. 1997. Fish biogeography and molecular clocks: perspectives from the Panamanian Isthmus. In: Kocher, T. D. & Stepien, C. A. (ed.), Molecular Systematics of Fishes. Academic Press, New York. p. 113–128.
- Brown, A. M. V. 2005. Molecular evolution, systematics and ecology of microsporidia from fishes and crustaceans. Ph.D. thesis, University of British Columbia, Vancouver, BC, 428 p.
- Brown, A. M. V. & Adamson, M. L. 2006. Phylogenetic Distance of *Theclohania butleri* Johnston, Vernick and Sprague, 1978 (Microsporidia; Thelohaniidae), a parasite of the Smooth Pink Shrimp *Pandalus jordani*, from its congeners suggests need for major revision of the genus *Theclohania* Henneguy, 1892. *J. Eukaryot. Microbiol.*, **53**: 445–455.
- Brown, A. M. V. & Kent, M. L. 2002. Molecular diagnostics for *Loma salmonae* and *Nucleospora salmonis* (microsporidia). In: Cunningham, C. O. (ed.), Molecular Diagnostics of Salmonid Diseases. Kluwer Academic Publishers, Dordrecht. p. 267–283.
- Cali, A. & Takvorian, P. M. 1999. Developmental morphology and life cycles of the microsporidia. In: Wittner, M. & Weiss, L. M. (ed.), The Microsporidia and Microsporidiosis. American Society for Microbiology Press, Washington, DC. p. 85–128.
- Canning, E. U. & Lom, J. 1986. The Microsporidia of Vertebrates. Academic Press, London. p. 1–289.
- Carr, S. M., Kivlichan, D. S., Pepin, P. & Crutcher, D. C. 1999. Molecular systematics of gadid fishes: implications for the biogeographic origins of Pacific species. *Can. J. Zool.*, **77**:19–26.
- Casal, G., Matos, E., Teles-Grilo, M. L. & Azevedo, C. 2009. Morphological and genetical description of *Loma psittaca* sp. n. isolated from the Amazonian fish species *Colomesus psittacus*. *Parasitol. Res.*, **105**:1261–1271.
- Cheney, S. A., Lafranchi-Tristem, N. J. & Canning, E. U. 2000. Phylogenetic relationships of *Pleistophora*-like microsporidia based on small subunit ribosomal DNA sequences and implications for the source of *Trachipleistophora hominis* infections. *J. Eukaryot. Microbiol.*, **47**: 280–287.
- Cheney, S. A., Lafranchi-Tristem, N. J., Bourges, D. & Canning, E. U. 2001. Relationships of microsporidian genera, with emphasis on the polyporous genera, revealed by sequences of the largest subunit of RNA polymerase II (RPB1). *J. Eukaryot. Microbiol.*, **48**:111–117.
- Cheynier, R., Kils-Hütten, L., Meyerhans, A. & Wain-Hobson, S. 2001. Insertion/deletion frequencies match those of point mutations in the hypervariable regions of the simian immunodeficiency virus surface envelope gene. *J. General. Virol.*, **82**:1613–1619.
- Cho, S., Mitchell, A., Regier, J. C., Mitter, C., Poole, R. W., Friedlander, T. P. & Zhao, S. 1995. A highly conserved nuclear gene for low-level phylogenetics: elongation factor-1 α recovers morphology-based tree for heliothine moths. *Mol. Biol. Evol.*, **12**:650–656.
- Corradi, N., Akiyoshi, D. E., Morrison, H. G., Feng, X. C., Weiss, L. M., Tzipori, S. & Keeling, P. J. 2007. Patterns of genome evolution among the microsporidian parasites *Encephalitozoon cuniculi*, *Antonospora locustae* and *Enterocytozoon bieneusi*. *PLoS ONE*, **2**, art. e1277.
- Docker, M. F., Devlin, R. H., Richard, J., Khattri, J. & Kent, M. L. 1997a. Sensitive and specific polymerase chain reaction assay for detection of *Loma salmonae* (Microsporea). *Dis. Aquat. Org.*, **29**:41–48.
- Docker, M. F., Kent, M. L., Hervio, D. M. L., Khattri, J. S., Weiss, L. M., Cali, A. & Devlin, R. H. 1997b. Ribosomal DNA sequence of *Nucleospora salmonis* Hedrick, Groff and Baxa, 1991 (Microsporea:Enterocytozoonidae): implications for phylogeny and nomenclature. *J. Eukaryot. Microbiol.*, **44**:55–60.
- Dogiel, V. A. 1936. Parasites of cod from the relic lake Mogilny. Annals of Leningrad University no.7 Biological Series. Problems of Ecological Parasitology p. 123–133.
- Diekmann, O. E., Bak, R. P. M., Stam, W. T. & Olsen, J. L. 2001. Molecular genetic evidence for probable reticulate speciation in the coral genus *Madracis* from a Caribbean fringing reef slope. *Mar. Biol.*, **139**:221–233.
- Dunn, A. M. & Smith, J. E. 2001. Microsporidian life cycles and diversity: the relationship between virulence and transmission. *Microbes Infect.*, **3**:381–388.
- Dunn, A. M., Terry, R. S. & Smith, J. E. 2001. Transovarial transmission in the microsporidia. *Adv. Parasitol.*, **48**:57–100.
- Fantham, H. B., Porter, A. & Richardson, L. R. 1941. Some microsporidia found in certain fishes and insects in eastern Canada. *Parasitology*, **33**:186–208.
- Faye, N., Toguebaye, B. S. & Bouix, G. 1995. On the cytology and development of *Loma booppsi* n. sp. (Microspora, Glugeidae), parasite of *Boops boops* (Pisces, Teleostei, Sparidae) from the coasts of Senegal. *Archiv Fur Protistenkunde*, **146**:85–93.
- Fomena, A., Coste, F. & Bouix, G. 1992. *Loma camerounensis* new species (Protozoa:Microsporida) a parasite of *Oreochromis niloticus* Linnaeus 1757 Teleostei Cichlidae in fish-rearing ponds in Melen Yaounde Cameroon. *Parasitol. Res.*, **78**:201–208.
- Goldman, N., Anderson, J. P. & Rodrigo, A. G. 2000. Likelihood-based tests of topologies in phylogenetics. *Syst. Biol.*, **49**:652–670.
- Hammer, O., Harper, D. A. T. & Ryan, P. D. 2001. PAST: paleontological Statistics software package for education and data analysis. *Palaeontol. Electronica*, **4**:1–9.
- Hauck, A. K. 1984. Mortality and associated tissue reactions of chinook salmon, *Oncorhynchus tshawytscha* (Walbaum), caused by the microsporidian *Loma* sp. *J. Fish Dis.*, **7**:217–229.
- Holmes, E. C., Worobey, M. & Rambaut, A. 1999. Phylogenetic evidence for recombination in dengue virus. *Mol. Biol. Evol.*, **16**:405–409.
- Huson, D. H. 1998. SplitsTree: analyzing and visualizing evolutionary data. *Bioinformatics*, **14**:68–73.
- Kabata, Z. 1959. On two little-known microsporidia of marine fishes. *Parasitology*, **49**:309–315.
- Kamaishi, T., Hashimoto, T., Nadamura, Y., Nakamura, F., Murata, S., Okada, N., Okamoto, K., Shimizu, M. & Hasegawa, M. 1996. Protein phylogeny of translation elongation factor EF-1 α suggests microsporidians are extremely ancient eukaryotes. *J. Mol. Evol.*, **42**: 257–263.
- Katinka, M. D., Duprat, S., Cronillot, E., Méténier, G., Thomarat, F., Preissner, G., Barbe, V., Peyrettaillade, E., Brottier, P., Wincker, P., Delbac, F., El Alaoui, H., Peyret, P., Saurin, W., Gouy, M., Weissenbach, J. & Vivarès, C. P. 2001. Genome sequence and gene compaction of the eukaryote parasite *Encephalitozoon cuniculi*. *Nature*, **414**: 450–453.
- Kent, M. L. & Speare, D. J. 2005. Review of the sequential development of *Loma salmonae* (Microsporidia) based on experimental infections of rainbow trout (*Oncorhynchus mykiss*) and Chinook salmon (*O. tshawytscha*). *Folia Parasitol.*, **52**:63–68.
- Kent, M. L., Elliot, D. G., Groff, J. M. & Hedrick, R. P. 1989. *Loma salmonae* (Protozoa: Microspora) infections in seawater-reared coho salmon *Oncorhynchus tshawytscha*. *Dis. Aquat. Org.*, **20**:231–233.
- Kent, M. L., Traxler, G. S., Kieser, D., Richard, J., Dawe, S. C., Shaw, R. W., Prosperi-Porta, G., Ketcheson, J. & Evelyn, T. P. T. 1998. Survey of salmonid pathogens in ocean-caught fishes in British Columbia, Canada. *J. Aquat. Anim. Health*, **10**:211–219.
- Khan, R. A. 2009. Parasites causing disease in wild and cultured fish in Newfoundland. *Icelandic Agric. Sci.*, **22**:29–35.
- Lipsitch, M., Siller, S. & Nowak, M. A. 1996. The evolution of virulence in pathogens with vertical and horizontal transmission. *Evolution*, **50**:1729–1741.
- Lom, J. 2002. A catalogue of described genera and species of microsporidians parasitic in fish. *Syst. Parasitol.*, **53**:81–99.
- Lom, J. & Laird, M. 1976. Parasitic protozoa from marine and euryhaline fish of Newfoundland and New Brunswick. II. Microsporida. *Trans. Am. Microsc. Soc.*, **95**:569–580.
- Lom, J. & Nilsen, F. 2003. Fish microsporidia: fine structural diversity and phylogeny. *Int. J. Parasitol.*, **33**:107–127.
- Lom, J. & Pekkarinen, M. 1999. Ultrastructural observations on *Loma acerinae* (Jirovec, 1930) comb. nov. (Phylum Microsporidia). *Acta Protozool.*, **38**:61–74.
- Loubès, C., Maurand, J., Gasc, C., de Buron, I. & Barral, J. 1984. Étude ultrastructurale de *Loma dimorpha* n. sp., microsporidie parasite de poissons Gobiidae languedociens. *Protistologica*, **14**:579–589.
- Lovy, J., Wright, G. M. & Speare, D. J. 2007. Ultrastructural examination of the host inflammatory response within gills of netpen-reared chinook salmon (*Oncorhynchus tshawytscha*) with microsporidial gill disease. *Fish Shellfish Immunol.*, **22**:131–149.
- Mallet, J. 1995. A species definition for the modern synthesis. *Trends Ecol. Evol.*, **10**:294–299.

- Morrison, C. M. 1983. The distribution of the microsporidian *Loma morhua* in tissues of the cod *Gadus morhua* L.. *Can. J. Zool.*, **61**:2155–2161.
- Morrison, C. M. & Marryatt, V. 1986. Further observations on *Loma morhua* Morrison & Sprague, 1981. *J. Fish Dis.*, **9**:63–67.
- Morrison, C. M. & Sprague, V. 1981a. Electron microscopical study of a new genus and new species of microsporidia in the gills of Atlantic cod, *Gadus morhua* L.. *J. Fish Dis.*, **4**:15–32.
- Morrison, C. M. & Sprague, V. 1981b. Light and electron microscope study of microsporidia in the gill of haddock, *Melanogrammus aeglefinus* (L.). *J. Fish Dis.*, **4**:179–184.
- Nemeczek, A. 1911. Beiträge zur Kenntnis der Myxo- und Microsporidien der Fische. *Arch. Protistenkd.*, **22**:143–169.
- Nilsen, F. & Chen, W. J. 2001. rDNA phylogeny of *Intrapredatorus barri* (Microsporidia: Amblyosporidae) parasitic to *Culex fuscans* Wiedemann (Diptera: Culicidae). *Parasitology*, **122**:617–623.
- O'Mahony, E. M., Tay, W. T. & Paxton, R. J. 2007. Multiple rRNA variants in a single spore of the microsporidian *Nosema bombi*. *J. Eukaryot. Microbiol.*, **54**:103–109.
- Ovcharenko, N. O., Sarabeev, V. L., Wita, I. & Czaplińska, U. 2000. *Loma mugili* sp. n., a new microsporidium from the gills of grey mullet (*Mugil soiuy*). *Vestnik zoologii*, **34**:9–15.
- Page, R. D. 1996. TreeView: an application to display phylogenetic trees on personal computers. *Comput. Appl. Biosci.*, **12**:357–358.
- Posada, D. & Crandall, K. A. 1998. MODELTEST: testing the model of DNA substitution. *Bioinformatics*, **14**:817–818.
- Putz, R. E., Hoffman, G. L. & Dunbar, C. E. 1965. Two new species of *Pleistophora* (Microsporidia) from North American fish with a synopsis of Microsporidia of freshwater and euryhaline fishes. *J. Protozool.*, **12**:228–236.
- Sánchez, J. G., Speare, D. J., Markham, R. J. F. & Jones, S. R. M. 2001a. Experimental vaccination of rainbow trout against *Loma salmonae* using a live low-virulence variant of *L. salmonae*. *J. Fish Biol.*, **59**:442–448.
- Sánchez, J. G., Speare, D. J., Markham, R. J. F. & Jones, S. R. M. 2001b. Isolation of a *Loma salmonae* variant: biological characteristics and host range. *J. Fish Biol.*, **59**:427–441.
- Sandeep, B. V. & Kalvati, C. 1985. A new microsporidian, *Loma trichiurini* sp., from the gill of a marine fish, *Trichiurus savala* Cuv. (Trichiuridae). *Indian J. Parasitol.*, **9**:257–259.
- Shaw, R. W. & Kent, M. L. 1999. Fish microsporidia. In: Wittner, M. & Weiss, L. M. (ed.), The Microsporidia and Microsporidiosis. American Society for Microbiology Press, Washington, DC. p. 418–446.
- Shaw, R. W., Kent, M. L. & Adamson, M. L. 2000a. Viability of *Loma salmonae* (Microsporidia) under laboratory conditions. *Parasitol. Res.*, **86**:978–981.
- Shaw, R. W., Kent, M. L. & Adamson, M. L. 2000b. Innate susceptibility differences in chinook salmon *Oncorhynchus tshawytscha* to *Loma salmonae* (Microsporidia). *Dis. Aquat. Org.*, **43**:49–53.
- Shaw, R. W., Kent, M. L. & Adamson, M. L. 2001. Phagocytosis of *Loma salmonae* (Microsporidia) spores in Atlantic salmon (*Salmo salar*), a resistant host, and chinook salmon (*Oncorhynchus tshawytscha*), a susceptible host. *Fish Shellfish Immunol.*, **11**:91–100.
- Shaw, R. W., Kent, M. L., Brown, A. M. V., Whipples, C. M. & Adamson, M. L. 2000c. Experimental and natural host specificity of *Loma salmonae* (Microsporidia). *Dis. Aquat. Org.*, **40**:131–136.
- Shaw, R. W., Kent, M. L., Docker, M. F., Brown, A. M. V., Devlin, R. H. & Adamson, M. L. 1997. A new species of *Loma* (Microsporea) in shiner perch (*Cymatogaster aggregata*). *J. Parasitol.*, **83**:296–301.
- Shimodaira, H. 2002. An approximately unbiased test of phylogenetic tree selection. *Syst. Biol.*, **51**:492–508.
- Shimodaira, H. & Hasegawa, M. 2001. CONSEL: for assessing the confidence of phylogenetic tree selection. *Bioinformatics*, **17**:1246–1247.
- Shulman, S. S. & Shulman-Albova, R. E. 1953. Fish Parasites of the White Sea. Izdatel'stvo AN SSSR, Moskva-Leningrad, Russia, 192 p.
- Sites, J. W. & Crandall, K. A. 1997. Testing species boundaries in biodiversity studies. *Conserv. Biol.*, **11**:1289–1297.
- Smith, J. E. 2009. The ecology and evolution of microsporidian parasites. *Parasitology*, **136**:1901–1914.
- Speare, D. J. & Daley, J. 2003. Failure of vaccination in brook trout *Salvelinus fontinalis* against *Loma salmonae* (Microspora). *Fish Pathol.*, **38**:27–28.
- Speare, D. J., Arsenault, G. J. & Buote, M. A. 1998. Evaluation of rainbow trout as a model for use in studies on pathogenesis of the branchial microsporidian *Loma salmonae*. *Contemp. Top. Lab. Anim. Sci.*, **37**:55–58.
- Speare, D. J., Brackett, J. & Ferguson, H. W. 1989. Sequential pathology of the gills of coho salmon with a combined diatom and microsporidian gill infection. *Can. Vet. J.*, **30**:571–575.
- Swofford, D. L. 2001. PAUP*. Phylogenetic Analysis Using Parsimony (*and Other Methods). Version 4. Sinauer Associates, Sunderland, MA.
- Tay, W. T., O'Mahony, E. M. & Paxton, R. J. 2005. Complete rRNA gene sequences reveal that the microsporidium *Nosema bombi* infects diverse bumblebee (*Bombus* spp.) hosts and contains multiple polymorphic sites. *J. Eukaryot. Microbiol.*, **52**:505–513.
- Templeton, A. R. 1994. The role of molecular genetics in speciation studies. In: Schierwater, B., Streit, B., Wagner, G. P. & DeSalle, R. (ed.), Molecular Ecology and Evolution: Approaches and Applications. Birkhäuser Verlag, Basel, Switzerland. p. 455–477.
- Thompson, J. D., Higgins, D. G. & Gibson, T. J. 1994. CLUSTAL W: improving the sensitivity of progressive multiple sequence alignment through sequence weighting, position specific gap penalties and weight matrix choice. *Nucleic Acids Res.*, **22**:4673–4680.
- Vossbrinck, C. R. & Debrunner-Vossbrinck, B. A. 2005. Molecular phylogeny of the Microsporidia: ecological, ultrastructural and taxonomic considerations. *Folia Parasitol.*, **52**:131–142.
- Vossbrinck, C. R., Maddox, J. V., Friedman, S., Debrunner-Vossbrinck, B. A. & Woese, C. R. 1987. Ribosomal RNA sequence suggests microsporidia are extremely ancient eukaryotes. *Nature*, **326**:411–414.
- Wheeler, Q. D. & Meier, R. 2000. Species Concepts and Phylogenetic Theory. Columbia University Press, New York, NY. p. 1–230.
- Williams, B. A. P. 2009. Unique physiology of host-parasite interactions in microsporidia infections. *Cell Microbiol.*, **11**:1551–1560.

SUPPORTING INFORMATION

Additional Supporting Information may be found in the online version of this article:

Table S1. Small subunit (SSU), internal transcribed spacer (ITS), large subunit (LSU) ribosomal DNA (rDNA), and elongation factor 1-alpha (EF-1 α) sequence characteristics for *Loma* species, showing alignment positions sequenced, intraspecific differences and total nucleotides sequenced across all isolates, clones or PCR products.

Table S2. Ribosomal DNA indels in *Loma* species in this study showing parsimony-informative interspecific indel sites (light shading) and parsimony-informative intraspecific indels (dark shading) (e.g. for *L. morhua* dashes at positions 1,381–1,387 indicate an indel that ranges from 0–4–6 nucleotides long depending on the isolate). Position numbers are relative to an *L. salmonae* reference sequence.

Table S3. Additive polymorphic rDNA sites in *Loma* species (i.e. those with three states, such as A and G, and both A and G), showing sites with only interspecific additivity (shared by two species) (light shading), sites with only intraspecific additivity (shared by at least two isolates per species) (dark shading), and sites with both inter- and intraspecific additivity (black shading). Most common state(s) are listed first. Degenerate code: R = (A and G), Y = (C and T), S = (C and G), W = (A and T), M = (C and A), K = (G and T).

Please note: Wiley-Blackwell are not responsible for the content or functionality of any supporting materials supplied by the authors. Any queries (other than missing material) should be directed to the corresponding author for the article.